USGS
science for a changing world

Surface Mineral Maps of Afghanistan Derived from HyMap Imaging Spectrometer Data, Version 2

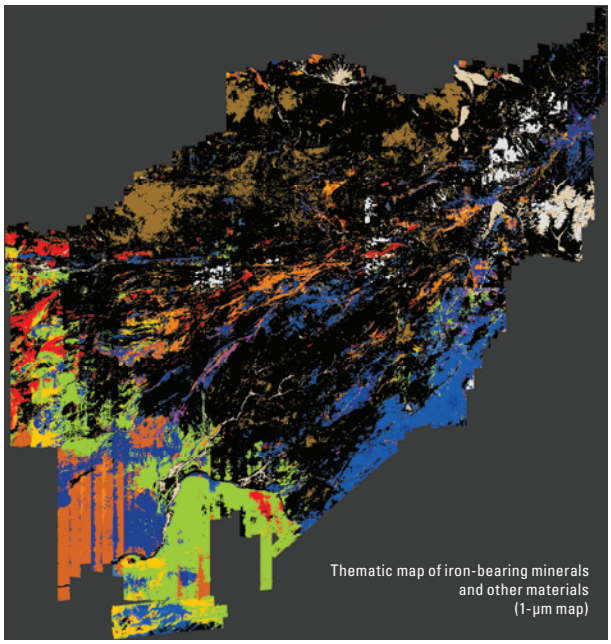

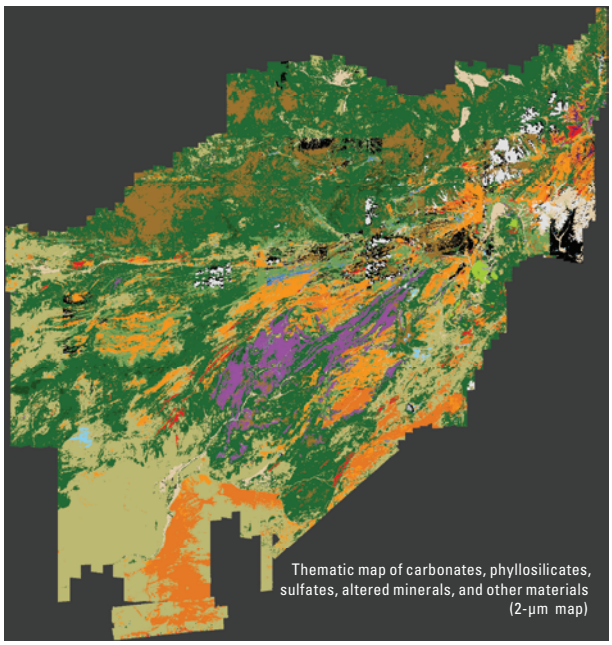

Data Series 787

USGS Afghanistan Project Product No. 186

U.S. Department of the Interior
U.S. Geological Survey

Surface Mineral Maps of Afghanistan Derived from HyMap Imaging Spectrometer Data, Version 2

By Raymond F. Kokaly, Trude V.V. King, and Todd M. Hoefen

Data Series 787

USGS Afghanistan Project Product No. 186

U.S. Department of the Interior
U.S. Geological Survey

U.S. Department of the Interior
SALLY JEWELL, Secretary

U.S. Geological Survey
Suzette M. Kimball, Acting Director

U.S. Geological Survey, Reston, Virginia: 2013

Suggested citation:
Kokaly, R.F., King, T.V.V., and Hoefen, T.M., 2013, Surface mineral maps of Afghanistan derived from HyMap imaging spectrometer data, version 2: U.S. Geological Survey Data Series 787, 29 p., http://pubs.usgs.gov/ds/787/.

Contents

Figures

Tables

Conversion Factors

Multiply	By	To obtain
	Length	
micrometer (μm)	1,000,000	meter (m)
meter (m)	3.281	foot (ft)
kilometer (km)	0.6214	mile (mi)
	Area	
square kilometer (km^2)	247.1	acre
square kilometer (km^2)	0.3861	square mile (mi^2)

Vertical coordinate information is referenced to WGS84 (EGM96) Vertical Datum

Horizontal coordinate information is referenced to the World Geodetic System Datum of 1984 (WGS-84)

Altitude, as used in this report, refers to distance above the vertical datum.

Surface Mineral Maps of Afghanistan Derived from HyMap Imaging Spectrometer Data, Version 2

By Raymond F. Kokaly, Trude V.V. King, and Todd M. Hoefen

Abstract

This report presents a new version of surface mineral maps derived from HyMap imaging spectrometer data collected over Afghanistan in the fall of 2007. This report also describes the processing steps applied to the imaging spectrometer data. The 218 individual flight lines composing the Afghanistan dataset, covering more than 438,000 square kilometers, were georeferenced to a mosaic of orthorectified Landsat images. The HyMap data were converted from radiance to reflectance using a radiative transfer program in combination with ground-calibration sites and a network of cross-cutting calibration flight lines. The U.S. Geological Survey Material Identification and Characterization Algorithm (MICA) was used to generate two thematic maps of surface minerals: a map of iron-bearing minerals and other materials, which have their primary absorption features at the shorter wavelengths of the reflected solar wavelength range, and a map of carbonates, phyllosilicates, sulfates, altered minerals, and other materials, which have their primary absorption features at the longer wavelengths of the reflected solar wavelength range. In contrast to the original version, version 2 of these maps is provided at full resolution of 23-meter pixel size. The thematic maps, MICA summary images, and the material fit and depth images are distributed in digital files linked to this report, in a format readable by remote sensing software and Geographic Information Systems (GIS). The digital files can be downloaded from *http://pubs.usgs.gov/ds/787/downloads/*.

Introduction

In 2007, imaging spectrometer data were acquired over most of Afghanistan to support assessments of natural resources and hazards in Afghanistan, as part of the U.S. Geological Survey (USGS) project "Oil and Gas Resources Assessment of the Katawaz and Helmand Basins." Imaging spectrometers measure the reflectance of the sun's radiation from the Earth's surface in many narrow channels. These sensors produce a reflectance spectrum for each image pixel, which can be interpreted to identify absorption features that arise from changes in the electron state of atoms, and vibrations in chemical and molecular bonds. Analyses of the positions and shapes of absorption features result in compositional information about minerals at the surface (Clark and others, 2003).

The HyMap imaging spectrometer (Cocks and others, 1998) was flown over Afghanistan in the fall of 2007 (Kokaly and others, 2008). Two maps indicating the distribution of surface minerals in Afghanistan were derived from the HyMap data and published (Kokaly and others, 2011; King and others, 2011a).

Purpose and Scope

This report describes the processing and analyses applied to the HyMap data to produce a revised set of maps of surface materials. In comparison to the first map release, the version 2 digital data are at full resolution and provided as digital files that can be imported into Geographic Information Systems (GIS) and image processing programs. By including additional reference spectra and adjusting detection thresholds, mineral discriminations are improved in version 2 compared to the original version. The data are provided in full resolution of 0.00020737 degree latitude by 0.00024753 degree longitude spacing (corresponding to 23 x 23 meter (m) pixel spacing).

Methodology

HyMap data were collected for most of Afghanistan in 2007. Following collection the data were processed through calibration, spectral analysis, and map production to produce a set of thematic maps: a map of iron-bearing minerals and other materials, and a map of carbonates, phyllosilicates, sulfates, altered minerals, and other materials.

Collection of HyMap Data

The HyMap imaging spectrometer has 512 cross-track pixels and covers the wavelength range of reflected sunlight, 0.43 to 2.48 microns (μm), with 128 sensor channels (Cocks and others, 1998). The imaging spectrometer was flown on

a WB-57 high-altitude aircraft at 15,240 m. There were 207 standard flight lines and 11 cross-cutting calibration lines collected over Afghanistan for a total of 218 flight lines (fig. 1), covering a surface area of more than 438,000 square kilometers (km^2) (Kokaly and others, 2008). The coverage spans approximately 860 kilometers (km) east to west and 900 km north to south. The data were collected on 28 separate flights (referred to as sorties) from August 22 to October 2, 2007.

The initial HyMap data were in scaled radiance form (calibrated to National Institute of Standards and Technology reference materials). Before subsequent processing, four channels that had low signal-to-noise ratios, were in wavelength regions overlapped by adjacent detectors, or both, were removed from the HyMap radiance data.

Processing of HyMap Data

The flow of processing HyMap data from radiance cubes to maps of surface minerals is illustrated in figure 2. First, HyMap radiance data were georectified, converted to reflectance, and further georeferenced to Landsat base imagery. These steps of the processing were done on an individual flight line basis. Data were then organized and mosaicked into image tiles, comprised, for the most part, of flight lines collected on a single day of acquisition.

Subsequent to forming image tiles, the HyMap reflectance data were analyzed with spectral analysis methods to determine the dominant material(s) present in each pixel of the HyMap image tiles. These images were further processed to detect clouds and define other material classes to produce summary images of surface materials. The processed image tiles grouped by flight date were then mosaicked together. The final surface mineral maps were formed by grouping spectrally similar mineral classes and other material classes together. These steps are described in detail in the following subsections.

Georeferencing

Each flight line was georectified using data from the HyMap on-board Global Positioning System (GPS) and inertial measurement unit (IMU). These data were further georeferenced to Landsat base imagery in Universal Transverse Mercator (UTM) projection (Davis, 2007). First order polynomial warping was used with nearest neighbor resampling in ENVI (ENvironment for Visualizing Images) version 4.7 (ITT Visual Information Solutions, 2009).

Reflectance Conversion

HyMap data were converted from radiance to reflectance using a multistep calibration process. This process removed the effect of the solar irradiance function, atmospheric absorptions, and residual instrument artifacts, resulting in reflectance spectra that have spectral features arising primarily from the material composition of the Earth's surface. Because of the extreme topographic relief (surface elevation in the part of the country with HyMap data spanned 280 to 5,642 m) and restricted access to ground-calibration sites, modifications to the standard USGS calibration procedures (Clark and others, 2002) were required to calibrate the 2007 Afghanistan HyMap dataset.

In the first step of the calibration process, the radiance data were converted to apparent surface reflectance using the radiative transfer correction program Atmospheric CORrection Now (ACORN) version 6lx (ImSpec LLC, Palmdale, California; http://www.imspec.com/index.html). ACORN was run multiple times for each flight line, using scene elevations in 100-m increments, covering the range of minimum to maximum elevation within the flight line. A single atmospherically corrected image was assembled from these elevation-incremented ACORN results. The image was formed by determining the elevation of each HyMap pixel and selecting the atmospherically corrected pixel from the 100-m increment closest to that elevation. The shuttle topographic radar mapping (SRTM) 90-m digital elevation model (DEM) was the elevation data source (U.S. Geological Survey, 2005).

Each assembled atmospherically corrected image was further empirically adjusted using ground-based reflectance measurements from a ground-calibration site. Ground-calibration spectra were collected from five different locales in Afghanistan: field spectra from Kandahar Air Field, Bagram Air Base, and Mazar-e-Sharif Airport (fig. 1), as well as laboratory spectra of samples from bare soil areas in Kabul and in Badakshan province (see the locations marked with green squares in fig. 1). At each site, the spectrum of the ground target was used to calculate an empirical correction factor for the airborne imaging spectrometer data. The correction factor was computed by dividing the field/laboratory spectrum of a ground-calibration site by the average spectrum of the ACORN-corrected HyMap pixels over the site. Subsequently, each spectrum in the HyMap flight lines was multiplied by the empirical correction factor from the nearest calibration site. This level of reflectance retrieval is termed radiative transfer ground-calibrated (RTGC) data (see Clark and others, 2002). Around the calibration site, RTGC data contain little atmospheric contamination and can be compared to laboratory spectra of mineral standards and field-measured reference spectra of vegetation (see the examples of such comparisons in Kokaly and others, 2009; Kokaly and others, 2007a, 2007b; Clark and others, 2003; and Kokaly and others, 2003); however, during the course of the airborne campaign, the sun angle, atmospheric water vapor content, and atmospheric scattering differed for each flight line. If the conditions in a flight line varied substantially from those at the nearest calibration site, residual atmospheric contamination was left in the RTGC data.

To remove the residual atmospheric contamination, cross-cutting calibration flight lines over the ground-calibration areas were acquired (fig. 1) and used to improve the reflectance calculation for standard data lines. A multiplier

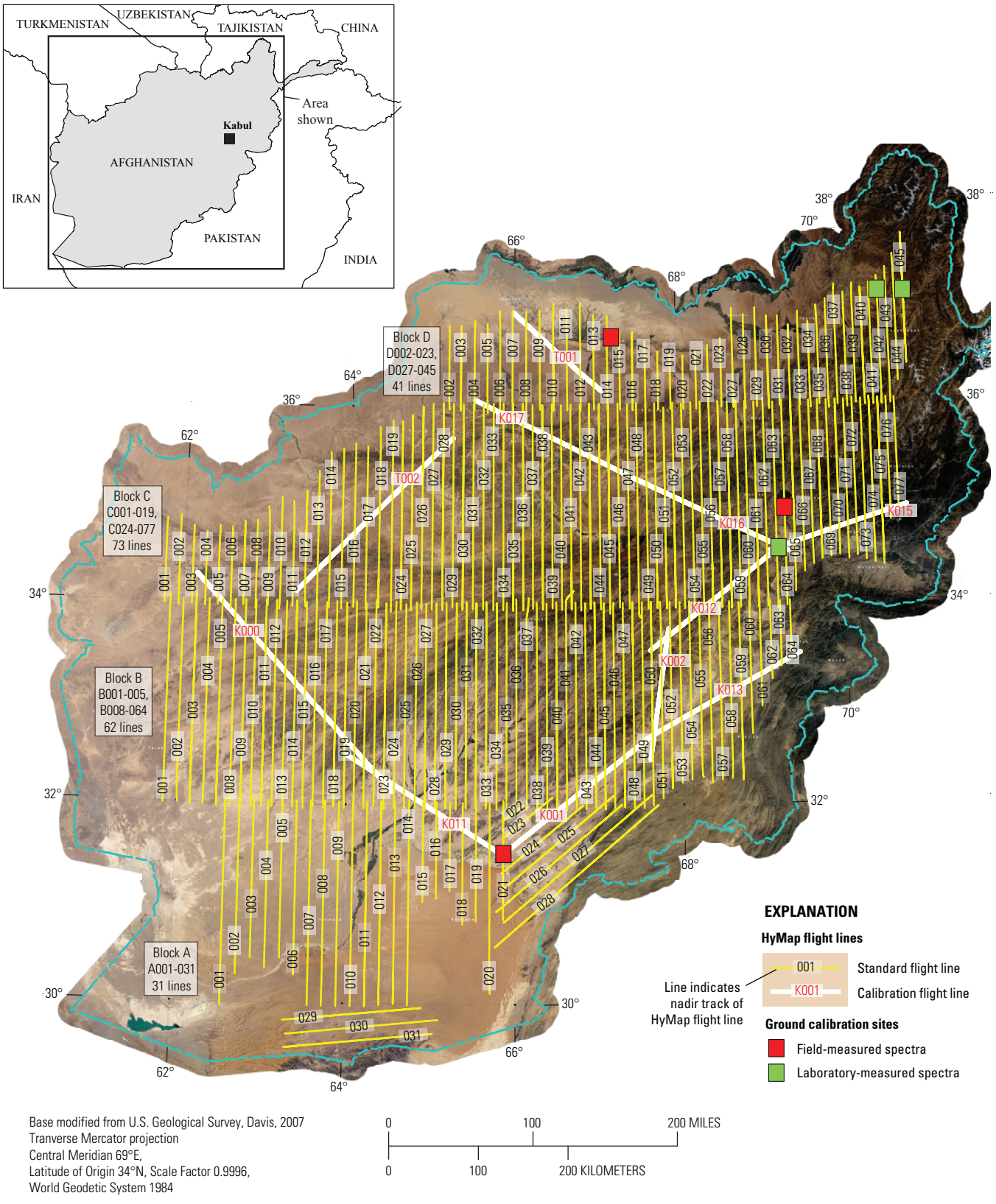

Figure 1. Flight lines of HyMap data collected over Afghanistan in 2007 (modified from Kokaly and others, 2008).

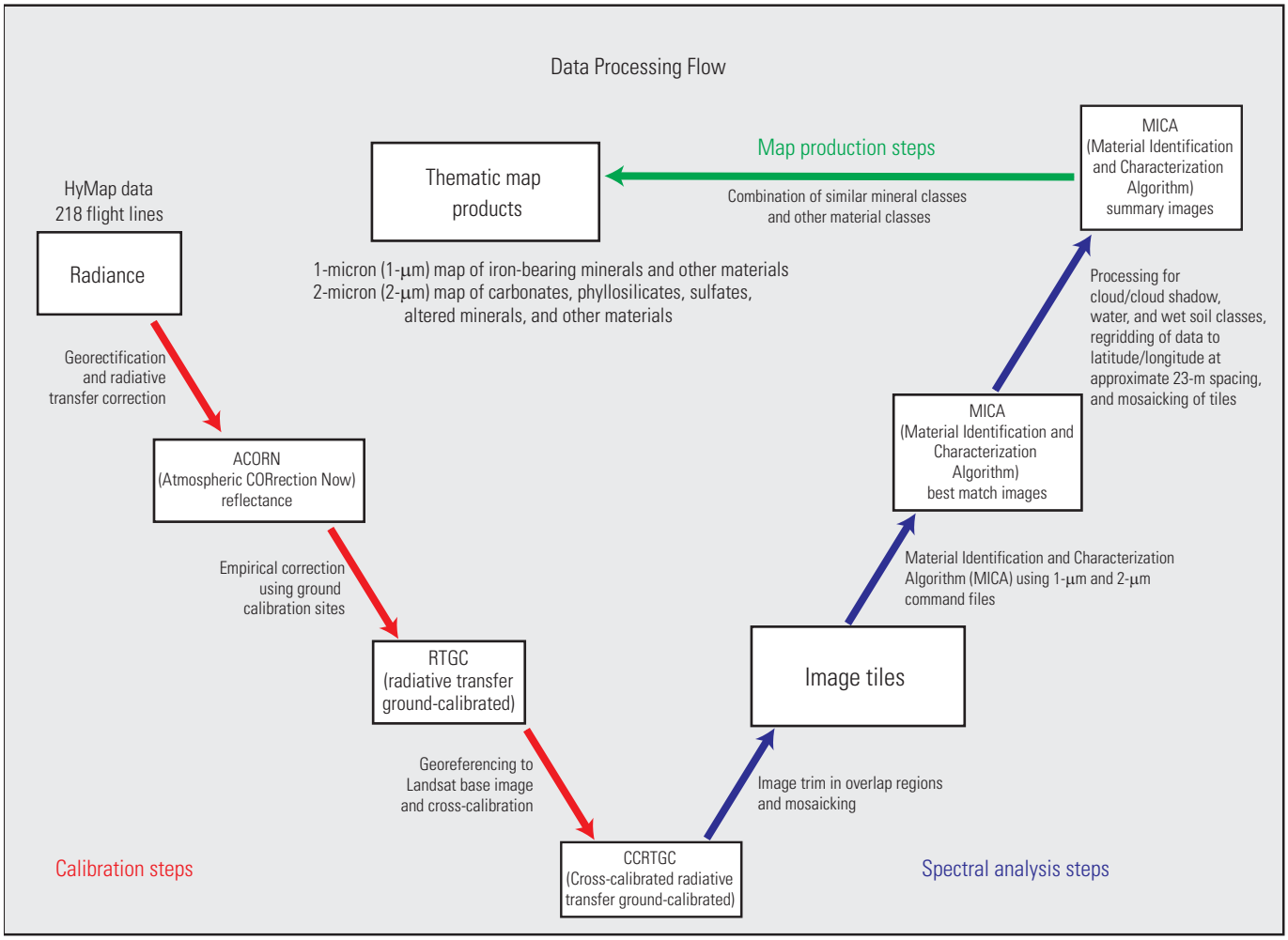

Figure 2. Processing steps applied to produce surface mineral maps from HyMap data.

correction for each standard data line, typically oriented in the north-south direction, was derived using the pixels of overlap with the well-calibrated cross-cutting lines. The overlapping pixels used in these calculations were restricted to shallow slopes and nonvegetated areas. Areas with strong, residual atmospheric contamination in the cross-cutting calibration line were not used. A correction factor was computed by dividing the average spectrum of the overlap pixels in the well-calibrated cross-cutting line by the average spectrum of the overlap pixels in the standard data line. After deriving the cross-calibration correction factor for a standard flight line, it was applied to every pixel in that flight line. These data are referred to as cross-calibrated RTGC data, or CCRTGC data.

A cloud and cloud-shadow detection algorithm was implemented to avoid mapping errors in cloud-contaminated pixels. The detection of cloud shadows was less accurate than cloud identification. Lower accuracy came, in part, from the decision to avoid potential false-positive detection of cloud shadows in areas of steep, north-facing, poorly illuminated slopes; as a result, cloud shadows were somewhat underdetected. Cloud contamination and strong elevation gradients in the area covered on sortie 13, flight lines C071-C077 (fig. 1) interfered with the cross-calibration method and parts of this tile were not well-calibrated to surface reflectance.

A large dust storm in southern Afghanistan blanketed the area covered on sortie 28, the last day of data collection, October 2, 2007. Flight lines A001-A006 and A015-019 were collected that day (see fig. 1). No correction for airborne dust, beyond the extension of the ground-calibration factor, was attempted. Thus, the spectra of those data likely contain an uncorrected contribution from airborne dust.

Image Tiling

Individual flight lines were mosaicked into 29 image tiles (fig. 3), where each tile primarily is composed of lines collected in one sortie (that is, on a single flight day). The exceptions were tiles B-2, B-3, B-9, C-3, C-6, and D-4, which were each composed of flight lines collected on two sorties. The dates of data collection for each sortie and the start and stop times of each flight line are given by Kokaly and others (2008), along with vector files containing the nadir tracks of the flight lines. Tiling was done to combine the 218 flight lines in the dataset into a more manageable number of parts. Daily

image tiles were selected because the flight lines on each day have fairly consistent atmospheric conditions, geographic location, and time of acquisition, all of which affect the reflectance retrieval. As data processing methods for this large dataset were developed, the organization of flight lines into daily image tiles facilitated the testing and refinement of atmospheric correction to produce the CCRTGC image tiles.

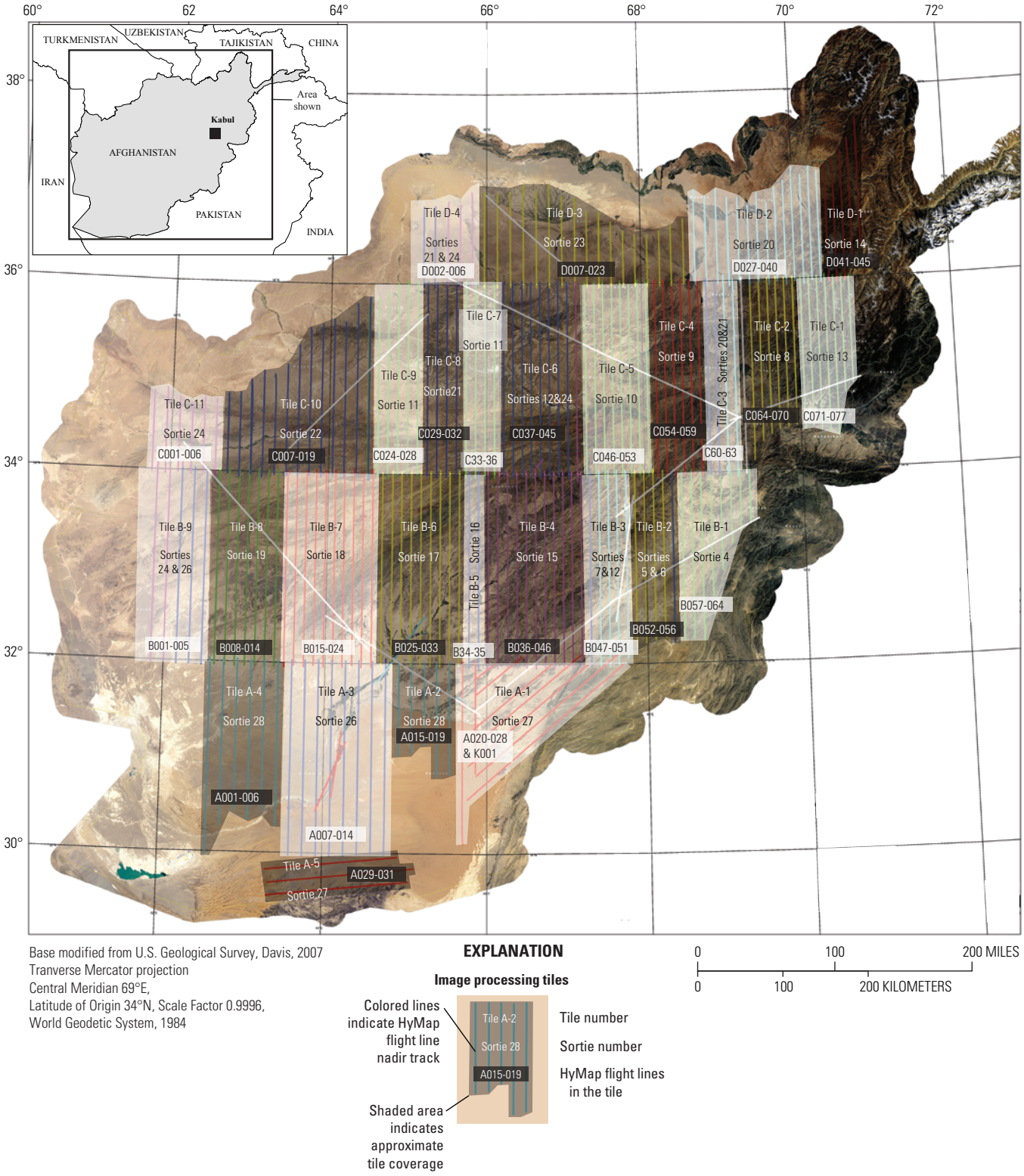

Figure 3. Image tiles formed from the HyMap flight lines.

Spectral Analysis and Material Identification

After completing the above procedures, CCRTGC image tiles were processed using the Material Identification and Characterization Algorithm (MICA; Kokaly, 2011). MICA, a program written in Interactive Data Language (IDL), is a module of the USGS PRISM (Processing Routines in IDL for Spectroscopic Measurements) software (Kokaly, 2011). MICA analysis identifies the mineral content in each pixel of imaging spectrometer data by comparing its reflectance spectrum to a reference spectral library of minerals, vegetation, water, and other materials. MICA and PRISM are available for download from *http://pubs.usgs.gov/of/2011/1155/*.

The MICA process is illustrated in figure 4 with a listing of the key inputs, analysis components, and outputs. MICA builds on the legacy of the USGS Tetracorder algorithm (Clark and others, 2003), with additional options for greater user control of feature weightings and identification constraints, and a greater ability to integrate program functions and image results with image processing and GIS software.

In MICA spectral comparisons, the term best match is applied to the reference spectrum that has the highest measure of similarity, in the wavelength positions and shapes of absorption features, between the reference spectra and the spectrum being analyzed (in this case, each pixel of imaging spectrometer data). The wavelength regions for the

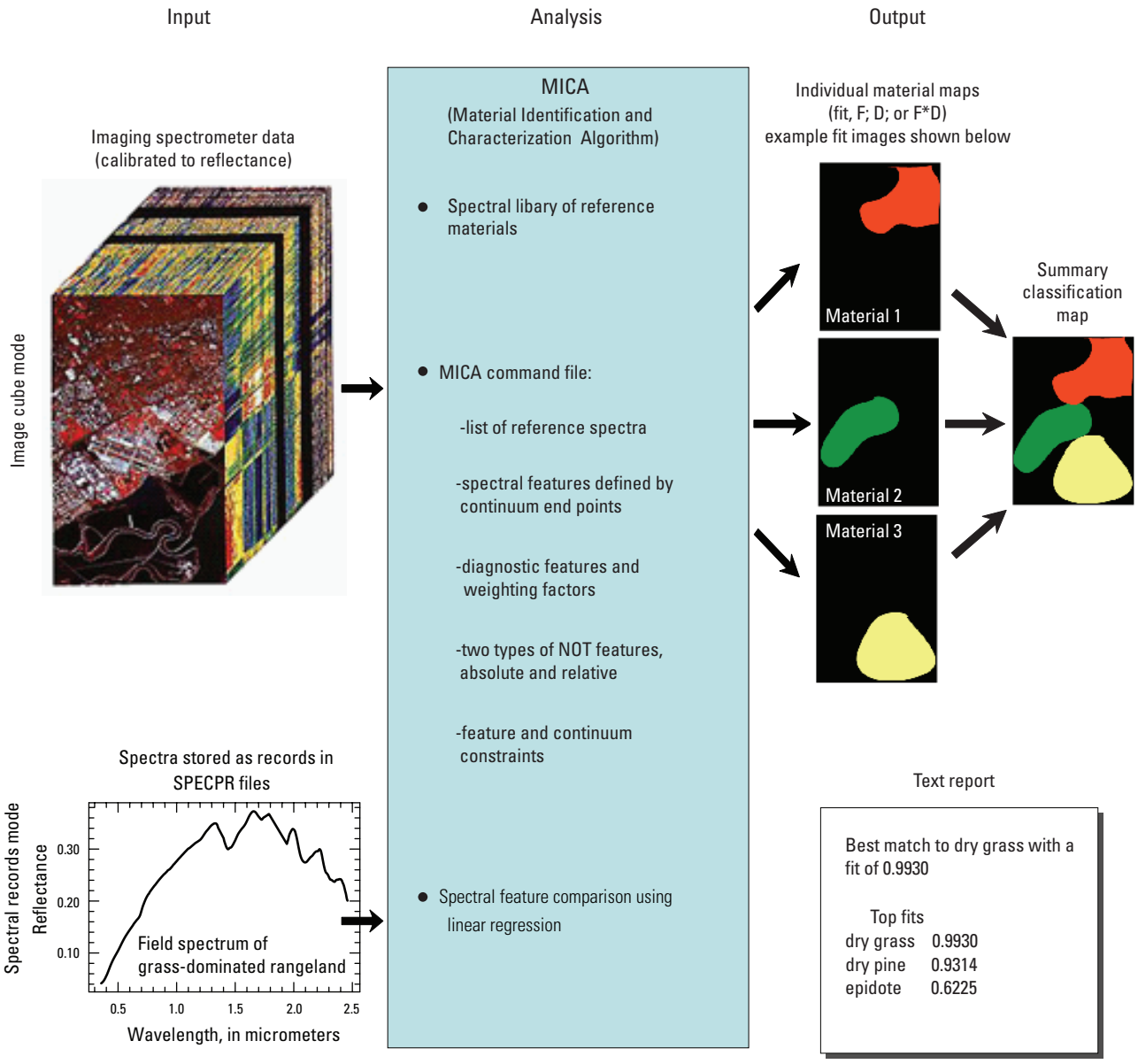

Figure 4. Processing flow and key elements of the Material Identification and Characterization Algorithm (MICA) image cube analysis (adapted from Kokaly, 2011).

comparisons are locations of diagnostic features in the reference spectra. Diagnostic features are strong features, unique features, or both, arising from chemical bonds inherent in the reference material. Continuum removal, or baseline normalization, is a method applied to isolate and analyze these diagnostic features (see Clark and Roush, 1984; Clark and others, 2003; and Kokaly and others, 2003) and commonly has been used in laboratory infrared spectroscopy (Ingle, 1988). This technique has been applied to terrestrial imaging spectrometer data as part of analyses to map the distribution of minerals and vegetation by comparing remotely sensed absorption band shapes to those in a reference spectral library (Clark and others, 1990; Clark and others, 2003; and Kokaly, 2011). The continuum is an estimate of the other absorptions present in the spectrum, not including the one of interest (Clark, 1999). In that sense, continuum removal is most often performed on absorption features. The values of the continuum-removed spectrum (R_C) are calculated by dividing the original reflectance values (R_O) by the corresponding values of the continuum line (R_L) for all the channels in the wavelength (λ) region of the absorption feature:

$$R_C(\lambda) = R_O(\lambda) / R_L(\lambda) \quad (1)$$

The depth (D) of the absorption feature at each channel is calculated by

$$D(\lambda) = 1 - R_C(\lambda) \quad (2)$$

An example of continuum removal applied to the pyrophyllite absorption feature in a HyMap pixel spectrum is shown in figure 5. A continuum-removed feature can be described by several parameters, including its central wavelength position and its depth at the band center. A feature's central wavelength position, commonly termed the band center, can be characterized in several ways (Kokaly, 2011) and here it is depicted at the wavelength of the channel at the minimum position in the continuum-removed feature (position of maximum depth) (fig. 5). The depth at the band center position of a feature is referred to as the band depth.

MICA uses the coefficient of determination (r^2) from the linear regression between a continuum-removed feature in the reference spectrum (fig. 5*B*-*C*) and corresponding continuum-removed region in the spectrum being analyzed (fig. 5*A*) as the feature fit value (F; a measure of the agreement between the spectral features). The r^2 fit value ranges from 0 to 1, with better matches indicated by high fit numbers and perfect similarity between spectral features indicated by a value of 1. A band depth for the feature being analyzed is computed using the reference feature scaled to the pixel spectrum. Values for band depth range from 0 to 1 for absorption features (dips in reflectance spectra). The reference feature scaled to the feature of the imaging spectrometer data is used instead of computing the depth directly to reduce the potential effect of noise in remotely sensed spectra (Kokaly, 2011 and Clark and others, 2003).

In MICA, the feature fits from multiple spectral features can be combined in a weighted average, where weighting factors can range from 0 to 1 and the sum of weights is constrained to equal 1. The weighted average is referred to as the overall fit or the material fit. In the MICA spectral comparisons, the best match is the reference spectrum with the highest overall fit value. Overall values for weighted depths are also computed during the MICA analysis. Example comparisons of a pixel spectrum from the HyMap data to several reference spectra are shown in figure 6. The best match for the pixel spectrum is to the pyrophyllite reference spectrum with a fit of 0.999. The next best matches were to reference spectra of linear mixtures of pyrophyllite with other minerals: pyrophyllite+alunite (in equal 50-percent proportions) and pyrophyllite+kaolinite (in 25-percent to 75-percent proportions), with overall fits of 0.802 and 0.768, respectively. Overall fits between the HyMap pixel's spectrum and the reference spectra of kaolinite+calcite (in 20-percent to 80-percent proportions) and alunite, were 0.673 and 0.667, respectively.

MICA uses optional feature and continuum constraints for each material to reduce false-positive identifications. Defined individually for each feature in reference spectra, the feature constraints are threshold levels on values of fit (F), depth (D), and fit multiplied by depth (F*D) that must be met by the spectrum being analyzed to consider it a match to the reference material. Similarly, continuum constraints for each feature must also be met by the spectrum being analyzed to consider it a match to the reference material, including thresholds on the reflectance levels of the left and right endpoints (R_{c1} and R_{c2}) and midpoint (R_{cmid}) of the continuum line, and the ratio of the reflectance levels of the continuum endpoints. The continuum and feature parameters subject to these constraints are depicted on the example HyMap spectrum in figures 5*B* and 5*C*. MICA also has the option of material constraints on fit, depth, and F*D for each reference spectra.

- The MICA fit, depth, and F*D analyses are controlled by user-edited text files called command files. These files include a listing of the reference spectra, diagnostic absorption features, continuum and feature constraints, and other parameters. The MICA command files used to produce the version 2 maps are included with the digital files distributed with this report (for instructions on how to access the digital data see the Data Files section of this report).

In this study, the HyMap data were compared to reference spectra of well-characterized mineral and material standards, including mixtures of minerals, which are available in version 6 of the USGS spectral library (Clark and others, 2007). MICA was applied to HyMap data twice to indicate the distribution of two categories of minerals that are naturally separated in the wavelength regions of their primary absorption features. A set of minerals with absorption features in the visible and near-infrared wavelength region were used to produce a map of iron-bearing minerals and other materials (King and others, 2011a), also referred to as the 1-μm map or the 1-micron map. A different set of minerals with absorption features in the shortwave infrared were used to produce a map of carbonates,

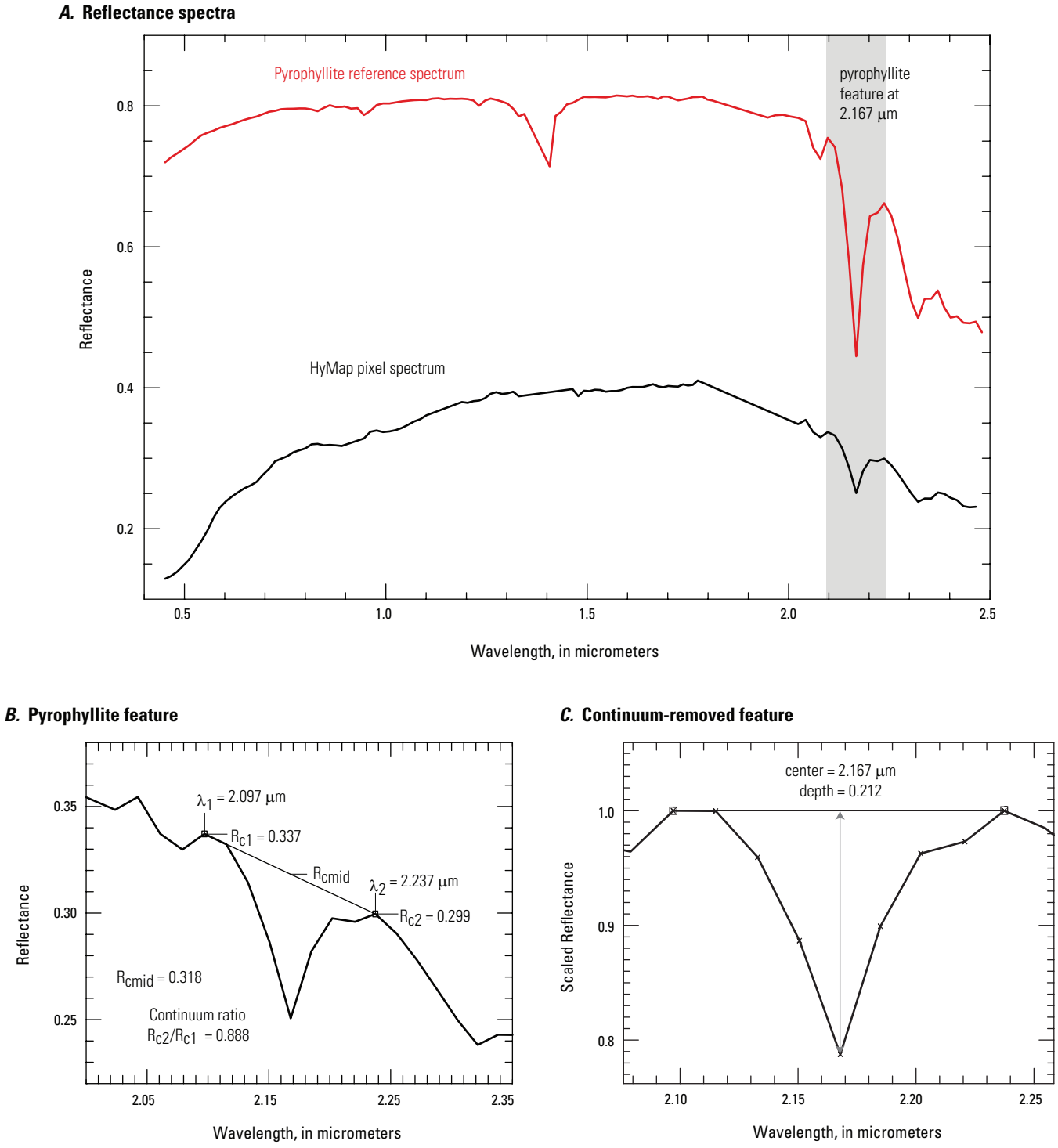

Figure 5. Continuum removal of pyrophyllite absorption feature in HyMap spectra: *A*, reference spectrum of pyrophyllite and HyMap spectrum; *B*, HyMap spectrum with continuum line (thin line) and continuum parameters; and *C*, continuum-removed pyrophyllite feature in HyMap spectrum and feature parameters (left and right endpoints (R_{c1} and R_{c2}) and midpoint (R_{cmid}) of the continuum line).

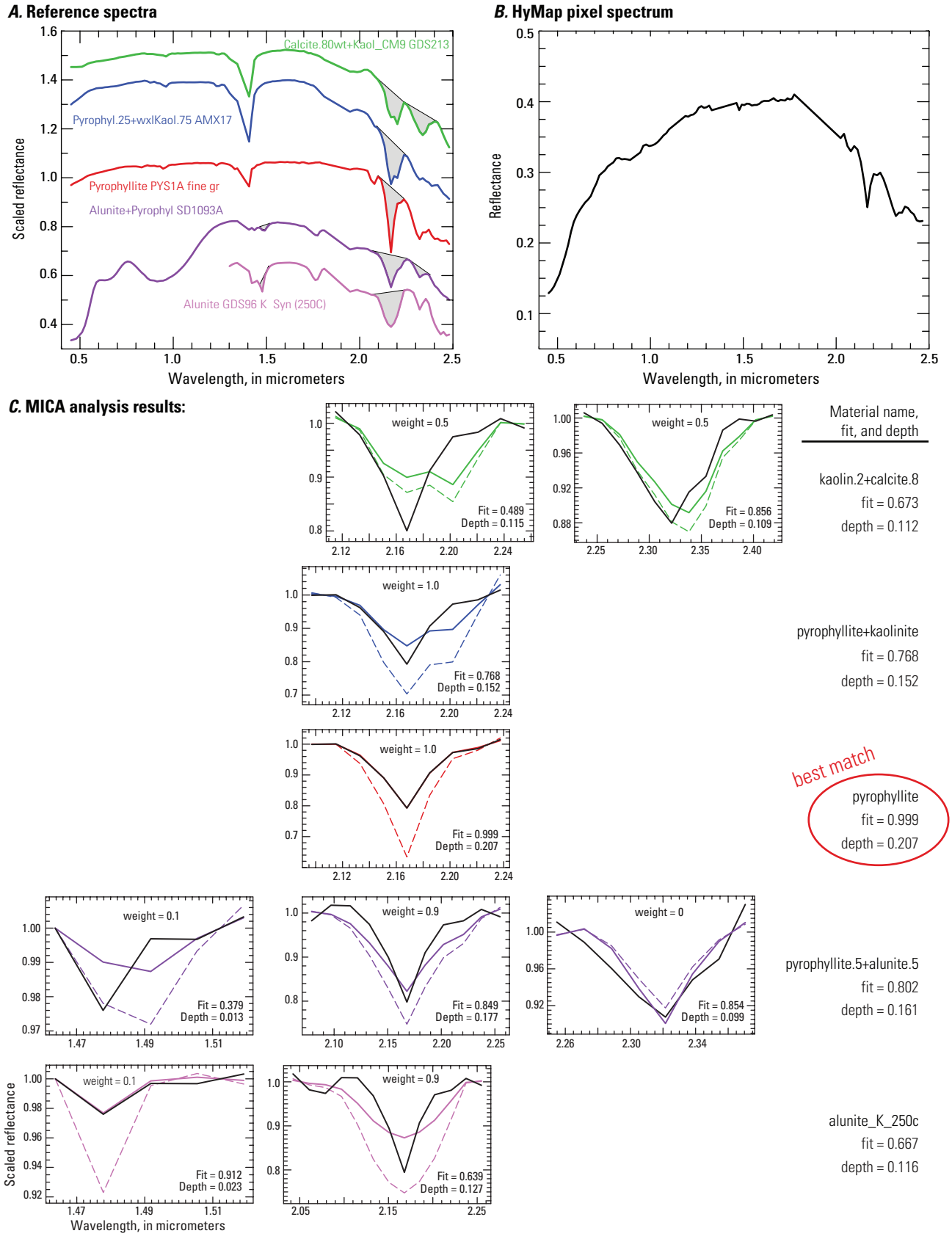

Figure 6. Spectral feature comparison of HyMap pixel with reference spectra. All unlabeled axes are scaled reflectance for the y-axis and wavelength, in micrometers, for the x-axis.

phyllosilicates, sulfates, altered minerals, and other materials (Kokaly and others, 2011), also referred to as the 2-µm map or 2-micron map. The reference spectra used in the MICA analyses to produce the 1-µm and 2-µm maps are shown in tables 1 and 2, respectively.

Several criteria guided the selection of reference spectra, including the expected reliability in detection and discrimination of material spectra at HyMap sensor characteristics; the importance of a material to studies of Afghanistan's geology, mineral resources, and soil composition; and the likelihood a material would be present in great enough abundance to be detected at the 23-m pixel size of the imagery. Another factor that was considered in the selection of reference spectra was atmospheric contamination, remnant in the reflectance data, which can hinder discrimination between minerals with similar spectral characteristics.

The summary output image from MICA is a classified image where each pixel has a value that indicates the reference spectrum that was determined to be the best match. Associated with the class value is the class name describing the material composition of the reference spectrum and a specific color assigned to represent that class (see columns 7 to 13 in tables 1 and 2). MICA analyses result in a not classified determination when absorption features of the reference spectra are not present in a pixel's spectrum. This can happen when the matches with reference spectra are poor and fall below threshold fit values for material detection or when the depth of detected absorption features are weak and fall below minimum threshold values for depth. For additional details on the factors that result in a not classified result refer to Kokaly (2011). Commonly, the MICA analysis of pixels in undetected cloud shadow areas gave a not classified result because their spectra have distorted spectral features caused by the shadowing effect of clouds. In these areas, pixels containing green vegetation and abundant carbonate minerals occasionally were identified because their spectra have strong absorption features.

Although extraordinary efforts were made to calibrate the HyMap data to reflectance, some areas of cloud-contaminated flight lines were difficult to convert to surface reflectance because water vapor variations were great along the length of these lines. As a result, small differences can sometimes be seen in the classification at the edges of flight lines containing clouds compared to adjacent flight lines. Similarly, minor differences in material classes are present between flight lines that were collected with greatly different sun angles. In particular, sortie 19 (corresponding to flight lines B008–B014 on fig. 1 and image tile B-8 on fig. 3) was flown late in the afternoon, 2:00–4:30 p.m. local time on September 21, 2007.

Combination of Classes into Thematic Maps

Following the MICA analysis, the summary output images for each tile were resampled to a geographic grid World Geodetic System 1984 (WGS-84) datum with 0.00020737 degree latitude by 0.00024753 degree longitude spacing (corresponding to a 23 x 23-m pixel grid). The tiles were mosaicked to create thematic maps of surface minerals for the full coverage of Afghanistan. In a similar manner, the corresponding material fit and depth image tiles were resampled and mosaicked. The final thematic maps derived from the MICA summary images are classified images where each pixel has a value that indicates the mineral class to which it belongs. Associated with the class value is the class name describing the mineral(s) represented by the class and a specific color assigned to represent that class (see columns 1 to 6 in tables 1 and 2).

For clarity of presentation in the thematic maps and consistency across the HyMap coverage, individual classes in the MICA summary images were bundled by combining reference spectra with similar spectral features. MICA results for reference spectra of the same mineral types, but with slight variations in mineral chemistry, were combined. For example, the results for calcium (Ca)-rich montmorillonite clay and the sodium (Na)-rich montmorillonite clay in the 2-µm MICA summary image were grouped into a single Montmorillonite class in the 2-µm thematic map. Other minerals in the 2-µm analysis that were combined in this manner include the muscovites, illites, kaolinites, alunites, and serpentines.

In other cases, distinct minerals with similar spectra were combined into a grouped class; for example, the combination of the results for the one epidote and two chlorite reference spectra into a single Epidote or chlorite class in the 2-µm thematic map. In a similar manner, the Hydrated silica class in the 2-µm thematic map is a combination of the MICA output classes for hydrated silica and opal reference spectra.

In some cases, classes were combined to indicate the presence of a particular mineral in combination with one or several minerals; for example, the Kaolinite and muscovite/clay/carbonate class, which combines the MICA output for six different mixtures of kaolinite with other minerals. These combinations were made to emphasize the distribution of a less frequently detected mineral with strong spectral character (in this example, kaolinite). Other examples of this type of combination include Calcite and clay/muscovite, Pyrophyllite (alunite or kaolinite may be present), and Buddingtonite. In the MICA summary images, the classes that comprise a combination in the thematic maps all have a similar color but with slight variation in brightness.

To produce the 1-µm thematic map of iron-bearing minerals and other materials, the MICA results for the reference spectra also were combined. Results for reference spectra of the same mineral types with slight variations in mineral chemistry were made to create the 1-µm thematic map classes of Jarosite and Chlorite. In addition to these combinations, reference spectra of the same mineral, with similar spectral features but different mineral grain size, were combined for hematite and goethite. Iron-bearing minerals with distinct mineral compositions, but also with similar broad spectral features spanning a wide wavelength range, were difficult to classify as unique mineral species across the full coverage of HyMap data. Thus, generic spectral classes, which combined several minerals with similar absorption features, were developed for

Table 1. Thematic map and summary image classes and reference spectra in the 1-micron (1-µm) Material Identification and Characterization Algorithm (MICA) analysis.

["*" indicates reclassified snow/ice pixels with greater than 3,150-m surface elevation; µm, micrometer]

1-µm thematic map						MICA 1-µm summary image						
Class names in final map	Class value in map	Color in map	Red	Green	Blue	Class names in MICA summary image	Class value in summary image	Color in summary image	Red	Green	Blue	Reference spectrum title
Not classified	0		0	0	0	Not_Classified	0		0	0	0	not applicable
Hematite, nanocrystalline	1		255	0	0	nanohematite.BR34b2	1		255	0	0	Nanohematite BR93-34B2 W1R1Bb
						hematite.thincoat	2		235	0	0	Hematite_Thin_Film GDS27 W1R1Ba
Hematite, fine-grained	2		215	0	0	hematite.finegr.fe2602	3		215	0	0	Hematite FE2602 W1R1Bb
Hematite, medium-grained	3		175	0	0	hematite.medgr.gds27	4		190	0	0	Hematite GDS27 W1R1Ba
						hematite.medgr.br25b	5		175	0	0	Hematite_Coatd_Qtz BR93-25B W1R1Bb
Hematite, coarse-grained	4		140	0	0	hematite.crsegr.br34c	6		155	0	0	Hematite_Coatd_Qtz BR93-34C W1R1Ba
						hematite.crsegr.br25c	7		140	0	0	Hematite_Coatd_Qtz BR93-25C W1R1Bb
Iron hydroxide	5		255	200	0	Fe-hydroxide	8		255	200	0	Fe-Hydroxide SU93-106 amorph W1R1Bb
Goethite, fine-grained	6		255	170	0	goethite.thincoat	9		255	185	0	Goethite_Thin_Film WS222 W1R1Ba
						goethite.finegr.mpcma2b	10		255	170	0	Goethite MPCMA2-B FineGr adj W1R1Bb
Goethite, medium-grained	7		240	130	0	goethite.medgr.ws222	11		240	150	0	Goethite WS222 Medium Gr. W1R1Ba
						goethite.medcrsegr.tracejarosite	15		240	130	0	Goethite MPCMA2-C M-Crsgrad2 W1R1Bb
						goethite+qtz.medgr.gds240	12		240	110	0	Goethite0.02+Quartz GDS240 W1R1Ba
Goethite, coarse-grained	8		215	100	0	goethite.coarsegr.ws222	13		215	100	0	Goethite WS222 Coarse Gr. W1R1Ba
						goethite.coarsergr.gds80	14		215	85	0	Lepidocrosite GDS80 (Syn) W1R1Bb
Goethite and jarosite	9		223	190	255	goethite+jarosite	16		223	190	255	Goeth+qtz.5+Jarosite.5 AMX11 W1R1Bb
Jarosite	10		218	112	214	jarosite.br34a2	17		218	112	214	Jarosite_on_Qtzite BR93-34A2 W1R1Bb
						jarosite_K200	18		208	102	204	Jarosite GDS99 K 200C Syn W1R1Ba
Fe^{2+} type 1	11		0	48	255	Fe2+_type_1a	19		0	48	255	Hypersthene NMNHC2368 W1R1Bb
						Fe2+_type_1b	20		0	38	245	Bronzite HS9.3B Pyroxene W1R1Bc
Fe^{2+} type 2	12		20	132	255	Fe2+_type_2a	21		20	132	255	Cummingtonite HS294.3B W1R1Bc
						Fe2+_type_2b	22		10	122	245	Diopside NMNHR18685 ~160 Pyx W1R1Bb
Fe^{3+} type 1	13		150	230	0	Fe3+_type_1a	23		150	230	0	Schwertmannite BZ93-1 W1R1Bb
						Fe3+_type_1b	24		140	220	0	Acid_Mine_Dr Assemb1-Fe3+ W1R1Fb
						Fe3+_type_1c	25		130	210	0	Acid_Mine_Dr Assemb2-Fe3+ W1R1Fb
Fe^{3+} type 2	14		125	170	0	Fe3+_type_2a	26		125	170	0	Desert_Varnish GDS78A Rhy W1R1Ba

Table 1. Thematic map and summary image classes and reference spectra in the 1-micron (1-µm) Material Identification and Characterization Algorithm (MICA) analysis.—Continued

["*" indicates reclassified snow/ice pixels with greater than 3,150-m surface elevation; µm, micrometer]

1-µm thematic map						MICA 1-µm summary image						
Class names in final map	Class value in map	Color in map	Red	Green	Blue	Class names in MICA summary image	Class value in summary image	Color in summary image	Red	Green	Blue	Reference spectrum title
						Fe3+_type_2b	27		115	160	0	Desert_Varnish GDS141 W1R1Ba
$Fe^{2+}Fe^{3+}$ type 1	15		0	60	150	Fe2+_Fe3+_type_1	28		0	60	150	Magnetite_skarn BR93-5B W1R1Bb
$Fe^{2+}Fe^{3+}$ type 2	16		0	90	180	Fe2+_Fe3+_type_2a	29		10	100	190	Chlorite+Muscovite CU93-65A W1R1Ba
						Fe2+_Fe3+_type_2b	30		0	90	180	Chlor+Goethite CU93-4B Phyl W1R1Ba
$Fe^{2+}Fe^{3+}$ type 3	17		25	190	255	Fe2+_Fe3+_type_3a	31		45	210	255	Olivine KI3291 Fo29 <60um W1R1Bb
						Fe2+_Fe3+_type_3b	32		35	200	255	Olivine GDS70.c Fo89 70um W1R1Bb
						Fe2+_Fe3+_type_3c	33		25	190	255	Olivine KI3054 Fo66 <60um W1R1Bb
Epidote	18		255	0	255	epidote	34		255	0	255	Epidote GDS26.a 75-200um W1R1Bb
Chlorite	19		199	0	255	chlorite_low_Fe	35		199	0	255	Chlorite SMR-13.b 60-104um W1R1Ba
						chlorite_high_Fe	36		189	0	245	Thuringite SMR-15.c 32um W1R1Ba
Maghemite	20		171	122	255	maghemite	37		171	122	255	Maghemite GDS81 Syn (M-3) W1R1Bb
Ferrihydrite	21		255	255	0	ferrihydrite	38		255	255	0	Ferrihydrite GDS75 Syn, F6 W1R1Bb
Green vegetation	22		225	205	170	vegetation1	39		225	205	170	Fir_Tree IH91-2 W1R1Ba
						vegetation.dry+green	40		220	200	165	Grass_dry.7+.3green AMX30 W1R1Ba
Dry vegetation	23		157	115	48	dry_veg_grass	41		162	120	53	Grass_Golden_Dry GDS480 W1R1Fa
						dry_veg_grass_2_3um	42		157	115	48	Grass_Golden_Dry GDS480 W1R1Fa
						dry_veg_nongrass	43		137	105	38	Lodgepole-Pine LP-Needles-3 W1R1Fa
						dry_veg_nongrass_2_3um	44		132	100	33	Lodgepole-Pine LP-Needles-3 W1R1Fa
Snow and ice	24		80	0	115	snow_melting	45		80	0	115	Melting_snow mSnw1a W1R1Fa
						snow_slush	46		75	0	110	Melting_snow mSnw9 (slush) W1R1Fa
Water	25		180	180	180	water	47		180	180	180	Seawater_Coast_Chl SW1 W1R1Ba
						water_sediment_low	48		175	175	175	Water+Montmor SWy-2+0.5g/l W1R1Fa
						water_sediment_high	49		170	170	170	Water+Montmor SWy-2+5.01g/l W1R1Fa
Wet soils*	26		140	140	140	Wet-Soil*	50		140	140	140	not applicable
No data	27		60	60	60	Nondata Pixel	51		60	60	60	not applicable
Cloud or cloud shadow	28		225	225	225	Cloud	52		255	255	255	not applicable

Table 2. Thematic map and summary image classes and reference spectra in the 2-micron (2-µm) Material Identification and Characterization Algorithm (MICA) analysis.

["*" indicates reclassified snow/ice pixels with greater than 3,150-m surface elevation; µm, micrometer]

2-µm thematic map						MICA 2-µm summary image						
Class names in final map	Class value in map	Color in map	Red	Green	Blue	Class names in MICA summary images	Class value in summary image	Color in summary image	Red	Green	Blue	Reference spectrum title
Not classified	0		0	0	0	not classified (image_unmapped_pixels)	0		0	0	0	not applicable
Calcite, abundant	1		20	75	0	calcite_abundant	1		20	75	0	Calcite WS272 W1R1Ba
Calcite	2		40	105	10	calcite	2		40	105	10	Calcite WS272 W1R1Ba
Calcite and muscovite/clay	3		113	160	90	calcite.7+muscovite.3	3		113	160	90	Calcite+.33Muscov AMX5 Ruby W1R1Ba
Calcite and clay/muscovite	4		188	185	115	calcite.8+montmorillonite_Ca.2	4		188	185	115	Calcite.8+Ca-Montmor.2 AMX15 W1R1Bb
						calcite.8+montmorillonite_Na.2	5		178	175	105	Calcite.80+Mont_Swy-1 GDS212 W1R1Ba
Carbonate and clay/muscovite	5		135	155	60	dolomite.25+calcite.25+mont_Na.5	9		135	155	60	Calc.25+dolo.25+mont.5 AMX18 W1R1Bb
Carbonate, iron-bearing	6		220	185	255	carbonate_Fe_bearing	6		220	185	255	Siderite HS271.3B W1R1Ba
Dolomite	7		205	25	255	dolomite	7		205	25	255	Dolomite HS102.3B W1R1Bb
Dolomite and clay/muscovite	8		165	20	200	dolomite.5+montmorillonite_Na.5	8		165	20	200	Dolomite.5+Na-mont.5 AMX21 W1R1Bb
Epidote or chlorite	9		225	25	0	epidote	10		215	15	0	Epidote GDS26.a 75-200um W1R1Bb
						chlorite_lowFe	11		225	25	0	Chlorite SMR-13.b 60-104um W1R1Ba
						chlorite+muscovite	12		245	45	20	Chlorite+Muscovite CU93-65A W1R1Ba
Muscovite	10		250	150	0	muscovite_lowAl	13		255	155	5	Muscovite CU93-1 low-Al Phyl W2R4Nb
						muscovite_medAl	14		250	150	0	Muscovite-medlowAl CU91-250A W1R1Fb
						muscovite_medhighAl	15		245	145	0	Muscovite GDS113 Ruby W1R1Bb
						muscovite_Fe-rich	16		240	140	0	Muscovite GDS116 Tanzania W1R1Ba
Illite	11		230	120	0	illite	17		230	120	0	Illite IMt-1.b <2um W1R1Ba
						illite_gds4	18		220	110	0	Illite GDS4 (Marblehead) W1R1Bb
Kaolinite (alunite, pyrophyllite or dickite may be present)	12		30	30	185	alunite.25+kaolinite.75	32		35	35	190	Kaolwxl.75+Alun_HS295 AMX14 W1R1Bb
						pyrophyllite+kaolinite	35		30	30	185	Pyrophyl.25+wxlKaol.75 AMX17 W1R1Bb
						kaol_possible_alunite_or_dickite	39		25	25	180	Dickite NMNH106242 W1R1Bb
Kaolinite	13		25	85	245	kaolinite_wxl	19		10	70	230	Kaolinite CM9 W1R1Bb
						kaolinite_pxl	20		25	85	245	Kaolinite KGa-2 (pxl) W1R1Bb
Kaolinite and muscovite/clay/carbonate	14		40	145	255	kaolin+clay_mica_or_halloysite	21		25	130	240	Halloysite NMNH106237 W1R1Ba
						kaolin.5+muscovite_medAl	22		30	135	245	Kaol.5+MuscCU91-250A AMX13 W1R1Bb
						kaolin+muscovite_mix_intimate	23		35	140	250	Kaol+Musc_intimate CU93-5C W1R1Ba
						kaolin.5+muscovite_medhighAl	24		40	145	255	Kaol_Wxl+0.5Musc_Ruby AMX12 W1R1Ba
						kaolin.5+smectite.5	25		45	150	255	Kaolin_Smect H89-FR-2 .5Kaol W1R1Bb
						kaolin.2+calcite.8	26		50	155	255	Calcite.80wt+Kaol_CM9 GDS213 W1R1Ba
Montmorillonite	15		130	210	255	montmorillonite_Na	27		130	210	255	Montmorillonite SWy-1 W1R1Bb
						montmorillonite_Ca	28		125	205	250	Montmorillonite SAz-1 W1R1Bb
Alunite	16		250	160	185	alunite_Na_450c	29		250	160	185	Alunite RES-3 Na Syn (450C) W2R4Na
						alunite_K_250c	30		245	155	180	Alunite GDS96 K Syn (250C) W2R4Na
Alunite and kaolinite	17		255	195	195	alunite.5+kaolinite.5	31		255	195	195	Alunite0.5+Kaol_KGa-1 AMX3 W1R1Bb

Table 2. Thematic map and summary image classes and reference spectra in the 2-micron (2-µm) Material Identification and Characterization Algorithm (MICA) analysis.—Continued

["*" indicates reclassified snow/ice pixels with greater than 3,150-m surface elevation; µm, micrometer]

2-µm thematic map						MICA 2-µm summary image						
Class names in final map	Class value in map	Color in map	Red	Green	Blue	Class names in MICA summary images	Class value in summary image	Color in summary image	Red	Green	Blue	Reference spectrum title
Pyrophyllite (alunite or kaolinite may be present)	18		145	25	55	pyrophyllite	33		145	25	55	Pyrophyllite PYS1A fine gr W1R1Ba
						pyrophyllite.5+alunite.5	34		155	35	65	Alunite+Pyrophyl SD1093A W1R1Bb
Jarosite	19		218	112	214	jarosite_Na	36		218	112	214	Jarosite GDS24 Na W1R1Bb
						jarosite_K	37		213	107	209	Jarosite GDS99 K 200C Syn W1R1Ba
						jarosite+muscovite_mix_intimate	38		208	102	204	Muscov+Jaros CU93-314 coatng W1R1Bb
Buddingtonite	20		255	210	0	buddingtonite	40		255	210	0	Buddingtonite GDS85 D-206 W1R1Bb
						buddingtonite+montmorillonite	41		245	200	0	Buddingtnt+Na-Mont CU93-260B W2R4Nb
Serpentine	21		160	215	50	serpentine1	42		160	215	50	Chrysotile HS323.1B W1R1Ba
						serpentine2	43		155	210	45	Antigorite NMNH96917.d 70um W1R1Bb
						serpentine3	44		150	205	40	Chrysotile HS323.1B W1R1Ba
						serpentine4	45		145	200	35	Antigorite NMNH96917.d 70um W1R1Bb
Serpentine, or dolomite and calcite	22		176	131	255	serpentine_or_dolomite+calcite	46		176	131	255	Antigorite NMNH96917.d 70um W1R1Bb
Tremolite or talc	23		100	40	180	tremolite_or_talc	47		100	40	180	Tremolite HS18.3 W1R1Bc
Hydrated silica	24		255	255	75	hydrated_silica	48		255	255	75	Opal TM8896 (Hyalite) W1R1Ba
						chalcedony	49		250	250	70	Chalcedony CU91-6A W1R1Ba
Gypsum	25		240	0	255	gypsum	50		240	0	255	Gypsum HS333.3B (Selenite) W1R1Ba
Green vegetation	26		225	205	170	vegetation_green	51		225	205	170	Fir_Tree IH91-2 W1R1Ba
						vegetation.dry+green	52		220	200	165	Grass_dry.7+.3green AMX30 W1R1Ba
Dry vegetation	27		157	115	48	dry_veg_grass	53		162	120	53	Grass_Golden_Dry GDS480 W1R1Fa
						dry_veg_grass_2_3um	54		157	115	48	Grass_Golden_Dry GDS480 W1R1Fa
						dry_veg_nongrass	55		137	105	38	Lodgepole-Pine LP-Needles-3 W1R1Fa
						dry_veg_nongrass_2_3um	56		132	100	33	Lodgepole-Pine LP-Needles-3 W1R1Fa
Snow and ice	28		80	0	115	snow_melting	57		80	0	115	Melting_snow mSnw1a W1R1Fa
						snow_slush	58		75	0	110	Melting_snow mSnw9 (slush) W1R1Fa
Water	29		180	180	180	water	59		180	180	180	Seawater_Coast_Chl SW1 W1R1Ba
						water_sediment_low	60		175	175	175	Water+Montmor SWy-2+5.01g/l W1R1Fa
						water_sediment_high	61		170	170	170	Water+Montmor SWy-2+0.5g/l W1R1Fa
Wet soils*	30		140	140	140	Wet-soil*	62		140	140	140	not applicable
No data	31		60	60	60	Non-data pixel	63		60	60	60	not applicable
Cloud or cloud shadow	32		225	225	225	Cloud	64		255	255	255	not applicable

the 1-µm thematic map, including the Fe^{3+} and Fe^{2+} classes and the combined Fe^{2+} Fe^{3+} classes.

Nonmineral classes were likewise combined in the 1-µm and 2-µm thematic maps. Multiple reference spectra for vegetation were used to capture the natural variability in vegetation spectral features that arise from biochemical composition differences. The two vegetation reference spectra with a chlorophyll absorption feature at 0.68 µm were combined into a single Green vegetation class. Since the nonphotosynthetic components of vegetation have absorption features in the shortwave infrared region of the electromagnetic spectrum (Elvidge, 1990; Kokaly and others, 2009), several reference spectra of dry, nonphotosynthetic vegetation were included in the MICA analyses and their results combined into a single Dry vegetation class in the 1-µm and 2-µm thematic maps. In a similar manner, the MICA best match results for multiple reference spectra of water were combined into a single class. The results from the MICA analyses indicated that bright, white soils were being identified as snow in playas where water had moistened the soil. Therefore, pixels identified as containing snow or ice and having an elevation at or below 3,150 m were re-classified as wet soil. Further examination in these areas revealed distortions in mineral spectral features because of the strong absorption features of water in the shortwave infrared. As a result, a vector file was created to identify areas in which spectra were affected by soil moisture. This file is available for download along with the maps at *http://pubs.usgs.gov/ds/787/downloads/*.

Thematic Maps of Surface Minerals

Iron-Bearing Minerals and Other Materials (1-µm Map)

The thematic map of iron-bearing materials and other materials (1-µm map) is depicted in figure 7. This figure and subsequent figures of the HyMap data are subsampled representations of the entire coverage (showing less than 1/600th of detail in the full resolution data). The corresponding MICA summary image of the full data coverage is not shown here; the reader is referred to the digital files to see the differences between the thematic map and the MICA summary image (for instructions on how to download the full resolution data layers see the Data Files section of this report). The fit image for the reference spectra detected using the 1-µm MICA command file for iron-bearing minerals and other materials is shown in figure 8. The variation in grayscale corresponds to variation from low fit values (dark pixels, indicating lower similarity to reference spectra) to high fit values (bright pixels, indicating higher similarity to reference spectra). The material depth image for the reference spectra detected using the 1-µm MICA command file for iron-bearing minerals and other materials is shown in figure 9. The variation in grayscale corresponds to variation from low depth values (dark pixels, indicating weak absorption features) to high depth values (bright pixels, indicating strong absorption features).

Carbonates, Phyllosilicates, Sulfates, Altered Minerals, and Other Materials (2-µm Map)

The thematic map of carbonates, phyllosilicates, sulfates, altered minerals, and other materials (2-µm map) is depicted in figure 10. As described for the 1-µm results, figure 10 and subsequent figures of the HyMap data are subsampled representations of the entire data coverage (for instructions on how to download the full resolution data layers see the Data Files section of this report). Thus, the MICA 2-µm summary image of the full data coverage is not shown because the differences between it and the thematic map cannot be adequately depicted on a page size figure.

A small part of the full resolution HyMap coverage of Afghanistan is shown in figure 11 to illustrate the detail of the dataset. The area shown in figure 11 is the Panjsher Valley area of interest (AOI), which is approximately 120 km northeast of Kabul. The AOI is known to have occurrences of and potential for emeralds and silver-bearing iron ores (Kokaly and Giles, 2011; Peters and others, 2007). In figure 11A, the single muscovite class of the thematic map is overlaid on a grayscale background. Figure 11B shows the various classes of muscovite with different aluminum compositions from the MICA 2-µm summary image. Thus, figure 11 shows how the additional classes in the MICA summary image can be used to see more detailed variations in surface mineralogy arising from slight changes in mineral chemistry.

The fit image for the reference spectra detected using the 2-µm MICA command file for carbonates, phyllosilicates, sulfates, altered minerals, and other materials is shown in figure 12. The variation in grayscale corresponds to variation from low fit values (dark pixels, indicating lower similarity to reference spectra) to high fit values (bright pixels, indicating higher similarity to reference spectra). The material depth image for the reference spectra detected using the 2-µm MICA command file for iron-bearing minerals and other materials is shown in figure 13. The variation in grayscale corresponds to variation from low depth values (dark pixels, indicating weak absorption features) to high depth values (bright pixels, indicating strong absorption features).

The material maps are being applied to natural resource development in areas of known potential mineralization (Peters and others, 2011). Previously unknown occurrences of minerals that suggest mineralization and potential targets for resource development, identified using the HyMap data, are beginning to be characterized and prioritized for further study (King and others, 2011b).

The reference spectra used in these analyses were an initial compromise between the level of detail achievable in the best calibrated flight lines and the discriminations that are robust, reliable, and perceptible at the scale (1:1,100,000) of

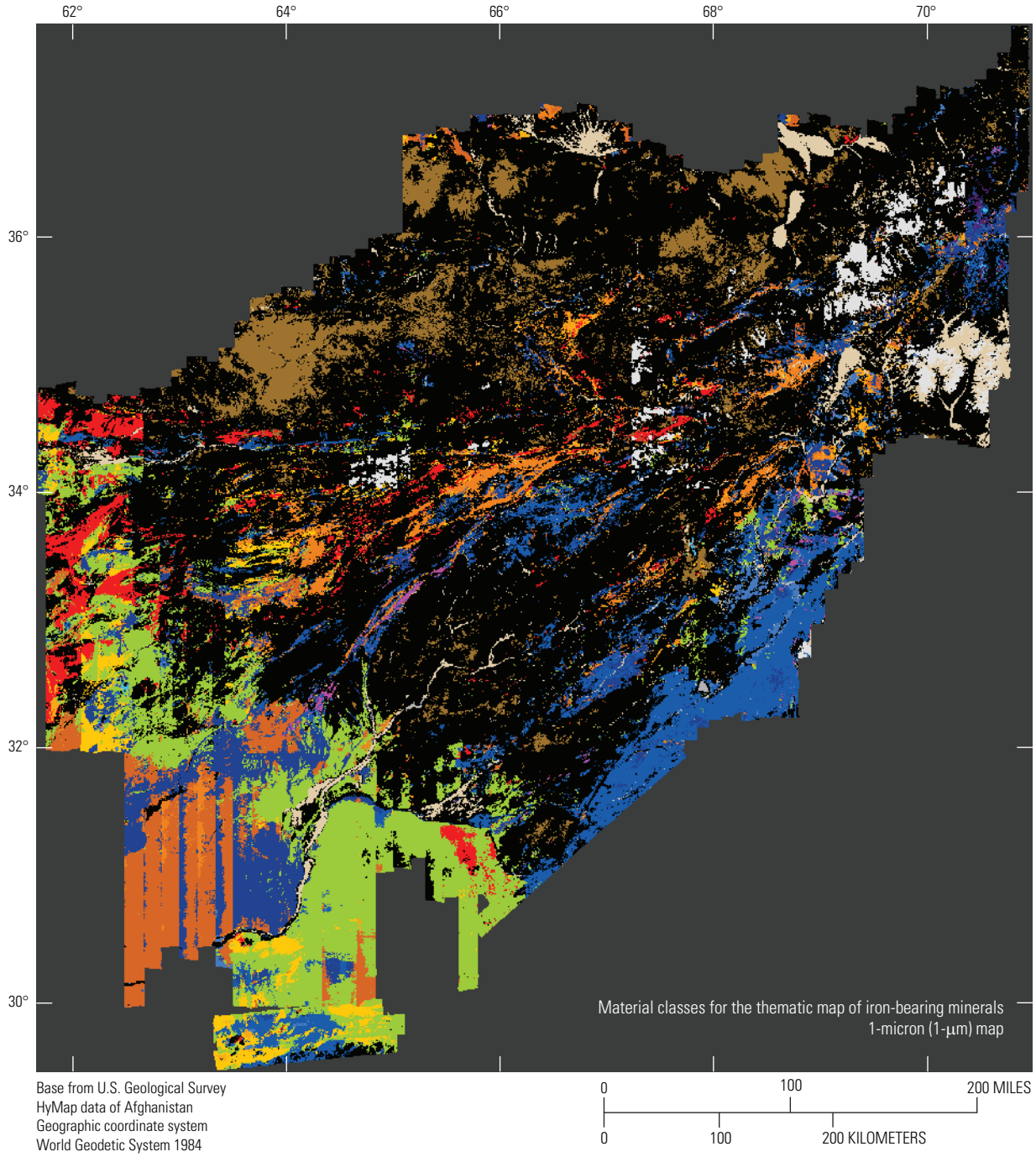

Figure 7. Thematic map of iron-bearing minerals and other materials (also referred to as the 1-micron or 1-μm map; see table 1 for all classes detected in the HyMap data).

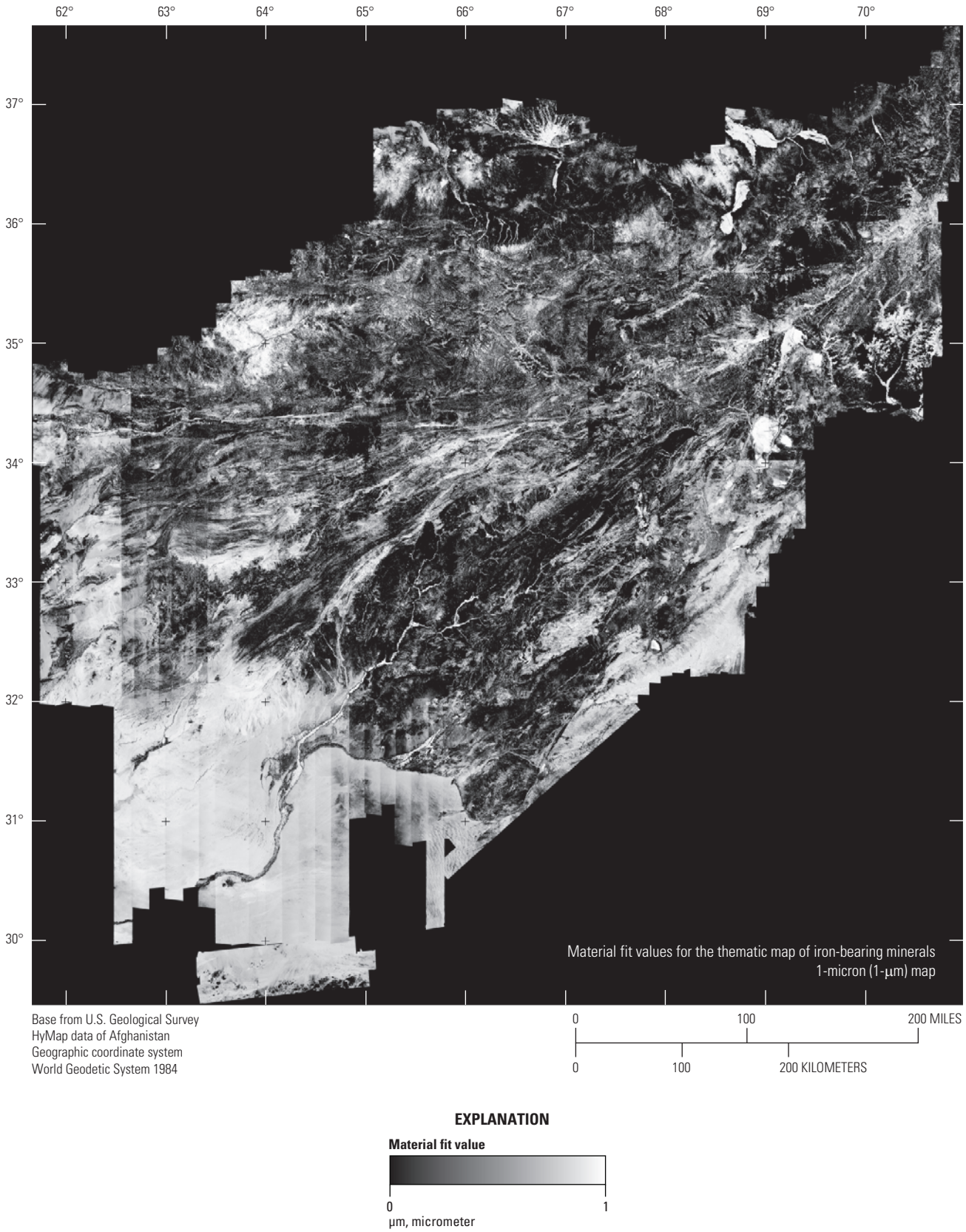

Figure 8. Material fit values for the 1-micron (1-μm) Material Identification and Characterization Algorithm (MICA) summary image (fit values of 0 to 1 stretched in gray scale from black to white). Pixels that do not contain data are depicted as black.

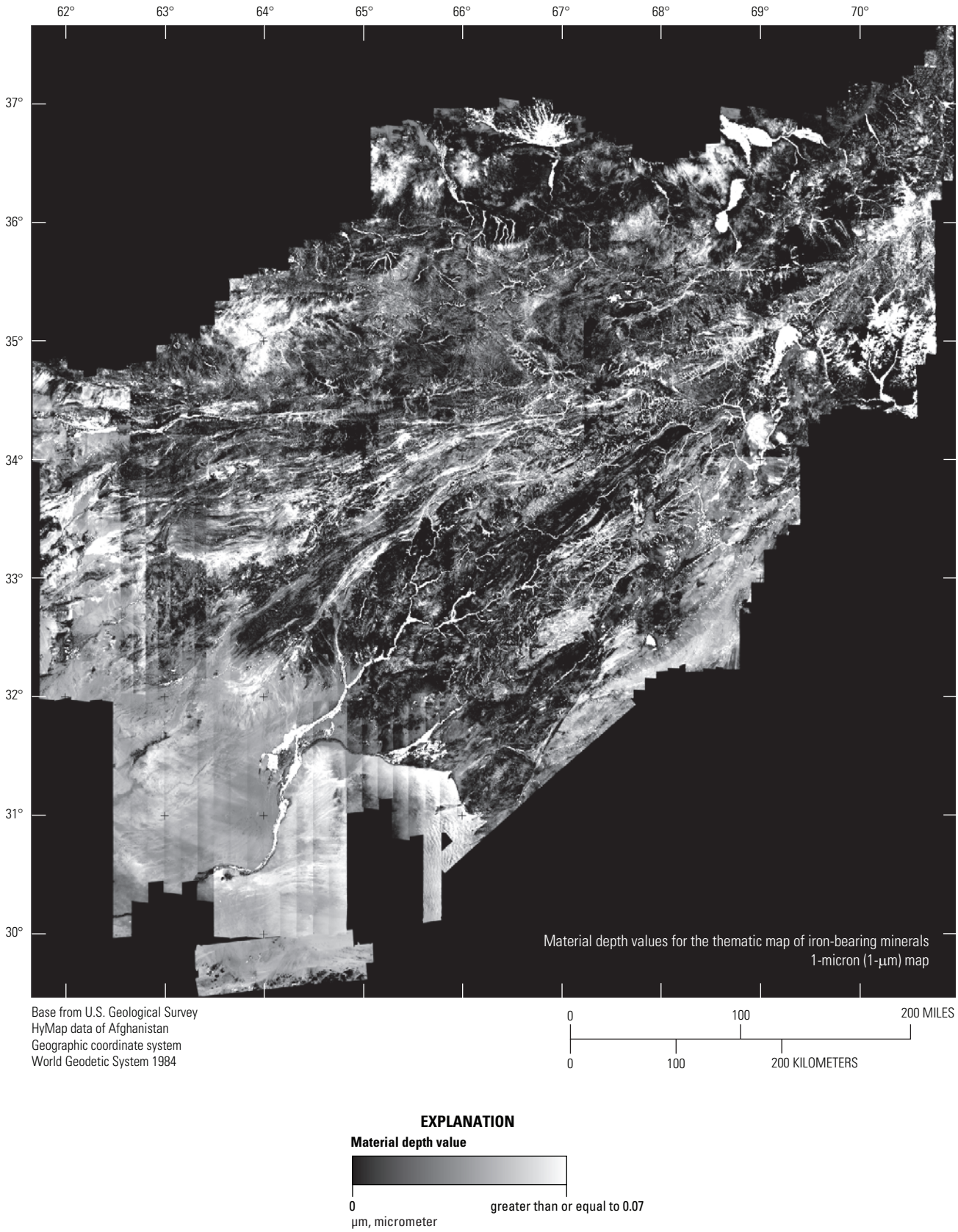

Figure 9. Material depth values for the 1-micron (1-μm) Material Identification and Characterization Algorithm (MICA) summary image (depth values of 0 to 0.07 stretched in gray scale from black to white, values above this range are depicted as white). Pixels that do not contain data are depicted as black.

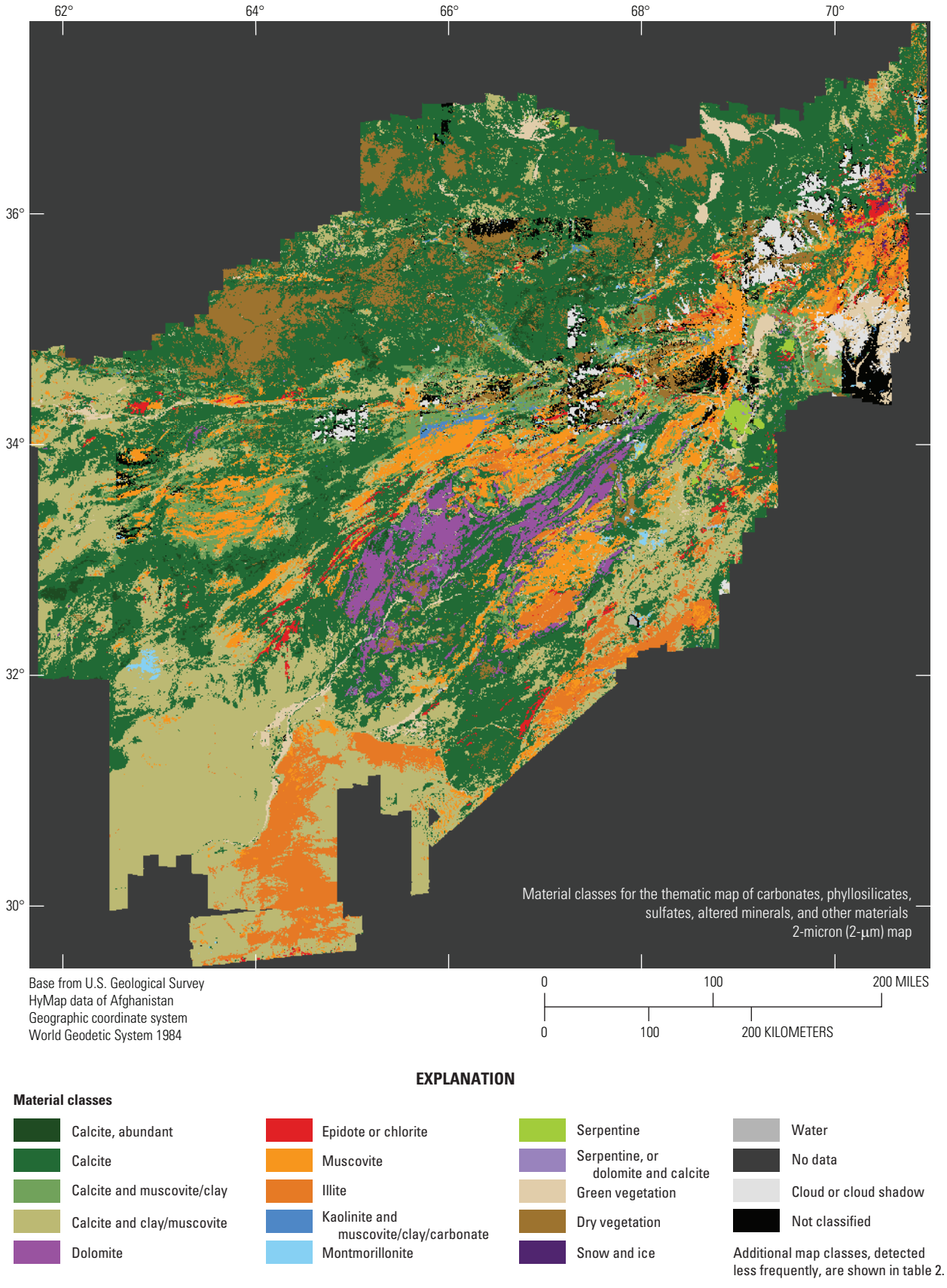

Figure 10. Thematic map of carbonates, phyllosilicates, sulfates, altered minerals, and other materials (also referred to as the 2-micron or 2-µm map; see table 2 for all classes detected in the HyMap data).

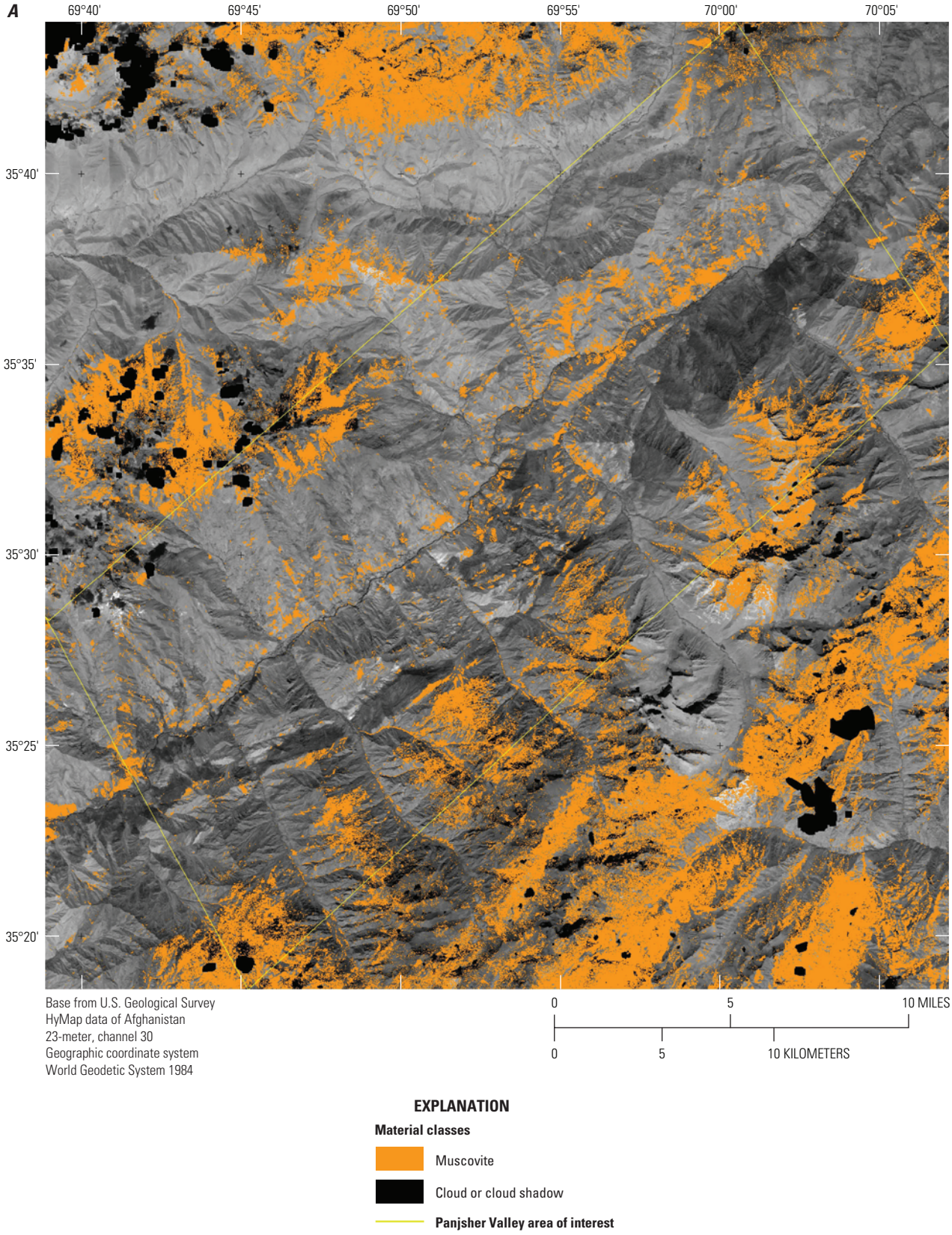

Figure 11. Muscovite mineral maps for the Panjsher Valley area of interest (see Kokaly and Giles, 2011): *A*, muscovite class from the 2-micron (2-μm) thematic map; and *B*, muscovite classes of varying aluminum content from the 2-μm Material Identification and Characterization Algorithm (MICA) summary image.

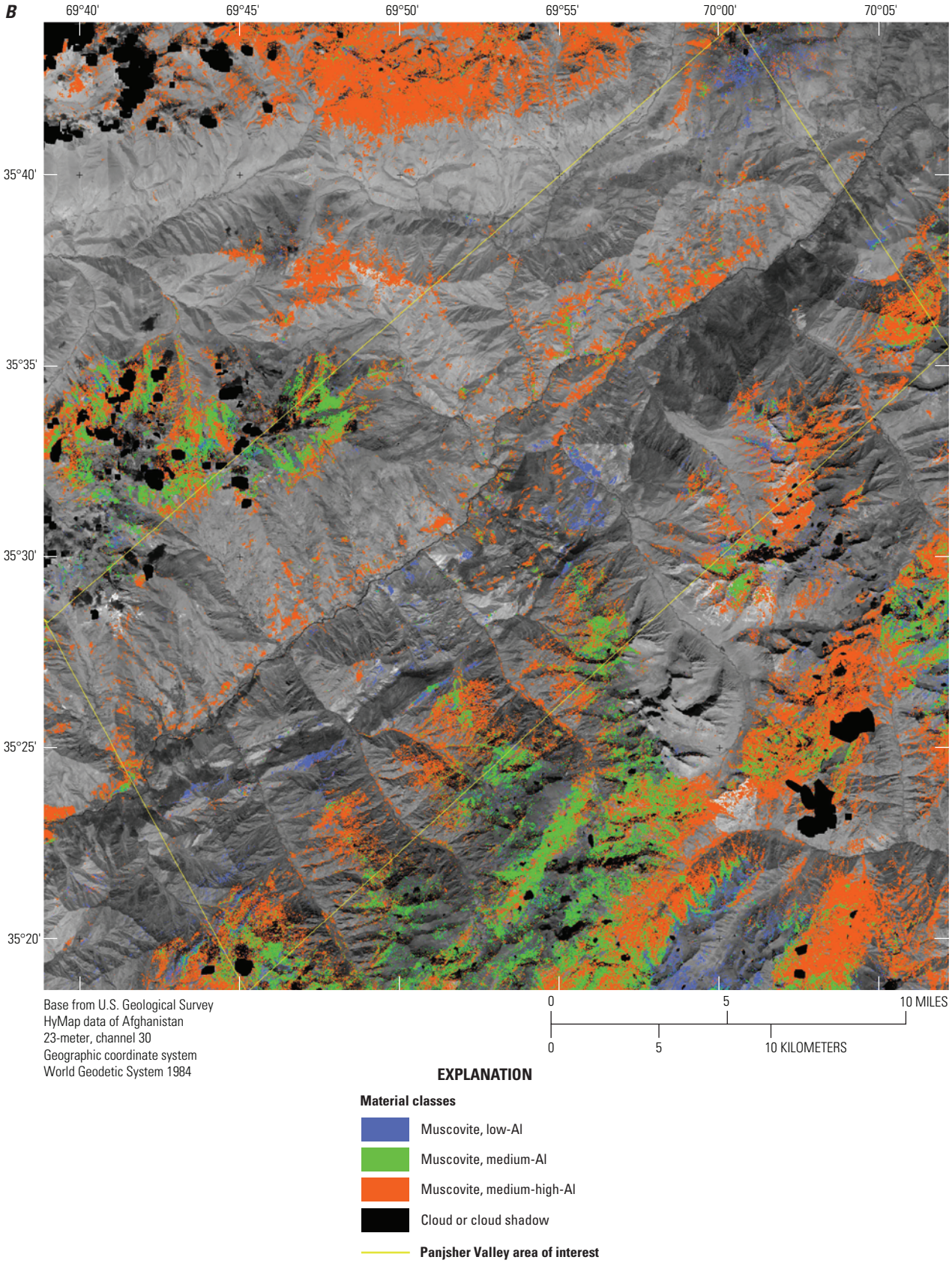

Figure 11. Muscovite mineral maps for the Panjsher Valley area of interest (see Kokaly and Giles, 2011): *A*, muscovite class from the 2-micron (2-μm) thematic map; and *B*, muscovite classes of varying aluminum content from the 2-μm Material Identification and Characterization Algorithm (MICA) summary image.—Continued.

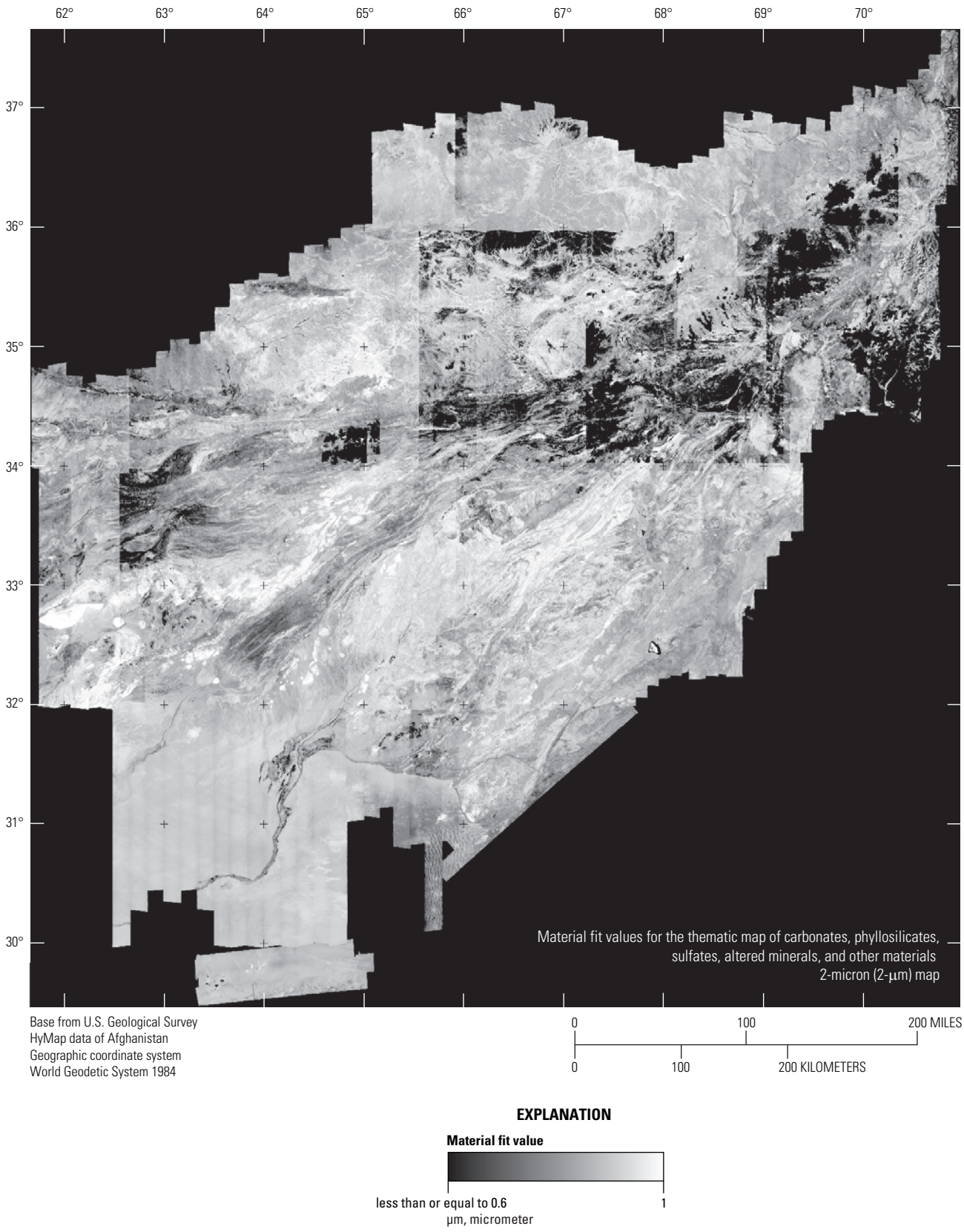

Figure 12. Material fit values for the 2-micron (2-μm) Material Identification and Characterization Algorithm (MICA) summary image (fit values of 0.6 to 1 stretched in gray scale from black to white, values below this range are depicted as black). Pixels that do not contain data are depicted as black.

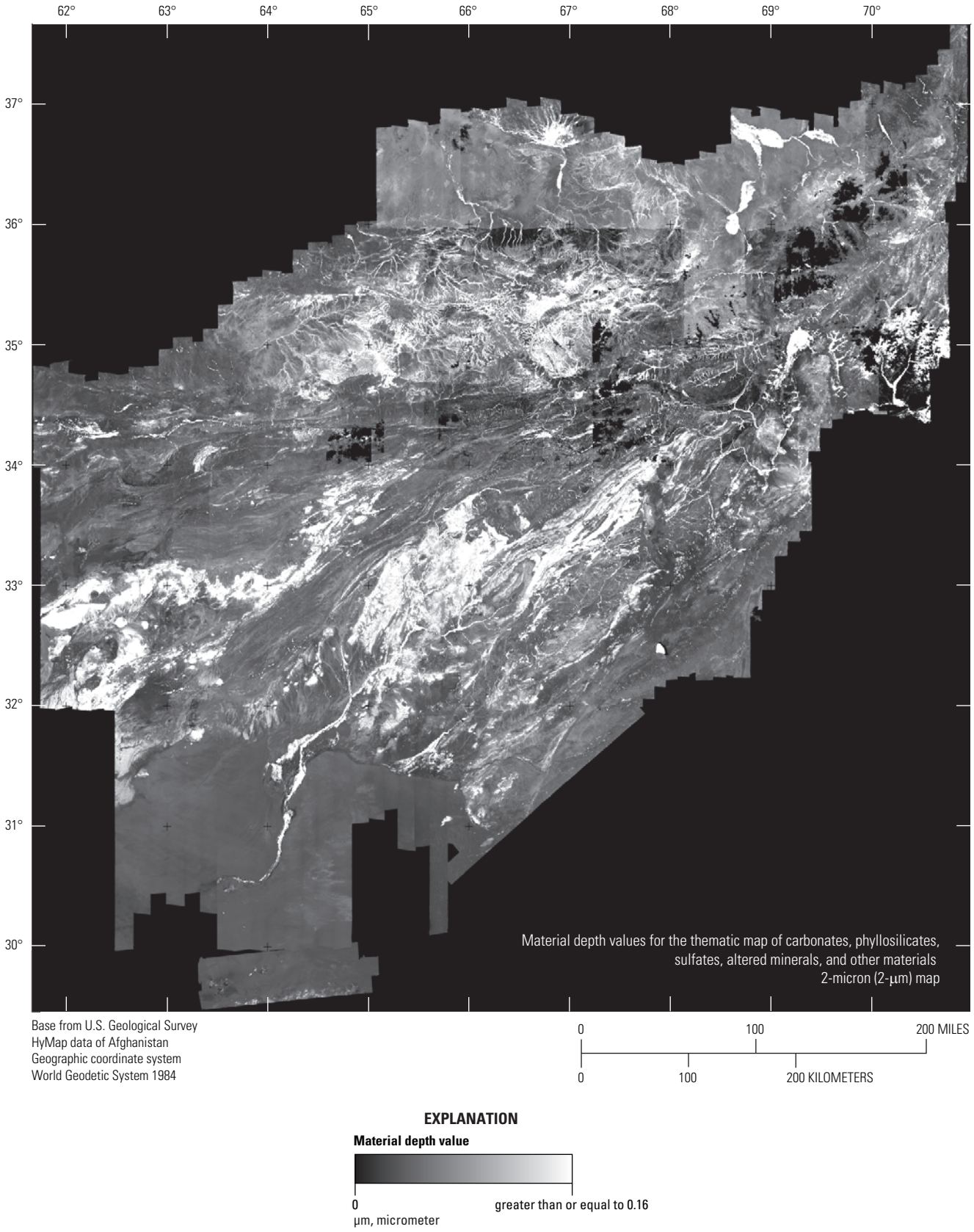

Figure 13. Material depth values for the 2-micron (2-μm) Material Identification and Characterization Algorithm (MICA) summary image (depth values of 0 to 0.16 stretched in gray scale from black to white, values above this range are depicted as white). Pixels that do not contain data are depicted as black.

the original version 1 maps. Future revisions of these digital mineral maps should consider the inclusion of additional spectra that may be present in small abundances across limited areas within specialized geologic environments, for example, rare earth minerals. Additional research into the spectral features in extensive regions of unclassified pixels in the 2-micron (2-µm) map should be made. By examining spectra in these areas, minerals that were not included in the reference spectra might be identified. Similarly, large contiguous areas with low fit values should also be examined to determine if the low fits are a result of a different mineral being present. Future calibration efforts should be targeted at areas in the maps where variation in mapped mineralogy is evident at image tile boundaries.

Data Files

Data files corresponding to the thematic maps of surface minerals, the MICA summary images of best match reference spectra, and material fit and depth images are provided with Federal Geographic Data Committee (FGDC) compliant metadata and are available at *http://pubs.usgs.gov/ds/787/downloads/*. Table 3 lists the files available for download along with their file formats. ENVI header files are included with the binary data files. These can be used to easily import the maps into remote sensing and GIS software (such as ENVI and ArcGIS). The raster data have dimensions of 37,679 image samples by 39,594 image lines. The data are in a geographic coordinate system referenced to the WGS84 datum. The coordinate of the center of the upper left pixel is 61.66019664 degrees east (E) longitude, 37.67081649 degrees north (N) latitude. Pixel spacing is 0.00024753 degrees longitude and 0.00020737 degrees latitude.

The vector file of areas affected by soil moisture also can be downloaded in either shapefile format or ENVI vector file format with FGDC-compliant metadata. The MICA command files used to generate the version 2 maps also are provided. These can be used with the MICA software to analyze imaging spectrometer data of other areas, with some adaptation required (Kokaly, 2011).

Table 3. Data files available for download.

[A '.dat' file extension was added to ENVI image file to work with ArcGIS. ENVI, ENvironment for Visualizing Images; MICA, Material Identification and Characterization Algorithm; µm, micrometer]

Data filename	Description	File format
afghan_thematicmap_1micron.dat	Classified map of iron-bearing minerals and other materials (1-µm thematic map)	Binary file of byte type. Image values correspond to minerals and other material classes as described in columns 1 – 6 of table 1. An associated ENVI header file (afghan_thematicmap_1micron.hdr) gives additional details on the file content.
afghan_thematicmap_1micron.hdr	ENVI header file for image file "afghan_thematicmap_1micron.dat"	Text file containing ENVI header information on the image file format.
afghan_thematicmap_1micron.xml	Metadata file for image file "afghan_thematicmap_1micron.dat"	Extensible Markup Language (XML) file describing the image file.
afghan_thematicmap_2micron.dat	Classified map of carbonates, phyllosilicates, sulfates, altered minerals, and other materials (2-µm map)	Binary file of byte type. Image values correspond to minerals and other material classes as described in columns 1 – 6 of table 2. An associated ENVI header file (afghan_thematicmap_2micron.hdr) gives additional details on the file content.
afghan_thematicmap_2micron.hdr	ENVI header file for image file "afghan_thematicmap_2micron.dat"	Text file containing ENVI header information on the image file format.
afghan_thematicmap_2micron.xml	Metadata file for image file "afghan_thematicmap_2micron.dat"	Extensible Markup Language (XML) file describing the image file.
MICAsummaryimage_1micron_classes.dat	Classified image of MICA output for iron-bearing minerals and other materials (MICA 1-µm summary image)	Binary file of byte type. Image values correspond to minerals and other material classes and reference spectra as described in columns 7 – 13 of table 1. An associated ENVI header file (MICAsummaryimage_1micron_classes.hdr) gives additional details on the file content.
MICAsummaryimage_1micron_classes.hdr	ENVI header file for image file "MICAsummaryimage_1micron_classes.dat"	Text file containing ENVI header information on the image file format.
MICAsummaryimage_1micron_classes.xml	Metadata file for image file"MICAsummaryimage_1micron_classes.dat"	Extensible Markup Language (XML) file describing the image file.
MICAsummaryimage_2micron_classes.dat	Classified image of MICA output for carbonates, phyllosilicates, sulfates, altered minerals, and other materials (MICA 2-µm summary image)	Binary file of byte type. Image values correspond to minerals and other material classes and reference spectra as described in columns 7 – 13 of table 2. An associated ENVI header file (MICAsummaryimage_2micron_classes.hdr) gives additional details on the file content.
MICAsummaryimage_2micron_classes.hdr	ENVI header file for image file "MICAsummaryimage_2micron_classes.dat"	Text file containing ENVI header information on the image file format.
MICAsummaryimage_2micron_classes.xml	Metadata file for image file "MICAsummaryimage_2micron_classes.dat"	Extensible Markup Language (XML) file describing the image file.
MICAsummaryimage_1micron_fits.dat	Image of fit values for iron-bearing minerals and other materials detected in the MICA 1-µm analysis	Binary file of signed integer type (Intel byte order). Image values correspond to fit values of the best match reference spectrum in each pixel. The fit value, which naturally ranges from 0 to 1, is scaled by a multiplication factor of 10,000 to save the image as integer data type to reduce file size. Refer to the class value of the corresponding pixel in the "MICAsummaryimage_1micron_classes" image and the information in columns 7 – 13 of table 1 to determine the best match material and reference spectrum of a pixel. An associated ENVI header file (MICAsummaryimage_1micron_fits.hdr) gives additional details on the file content.
MICAsummaryimage_1micron_fits.hdr	ENVI header file for image file "MICAsummaryimage_1micron_fits.dat"	Text file containing ENVI header information on the image file format.
MICAsummaryimage_1micron_fits.xml	Metadata file for image file "MICAsummaryimage_1micron_fits.dat"	Extensible Markup Language (XML) file describing the image file.

Table 3. Data files available for download.—Continued

[A '.dat' file extension was added to ENVI image file to work with ArcGIS. ENVI, ENvironment for Visualizing Images; MICA, Material Identification and Characterization Algorithm; µm, micrometer]

Data filename	Description	File format
MICAsummaryimage_2micron_fits.dat	Image of fit values for carbonates, phyllosilicates, sulfates, altered minerals, and other materials detected in the MICA 2-µm analysis	Binary file of signed integer type (Intel byte order). Image values correspond to fit values of the best match reference spectrum in each pixel. The fit value, which naturally ranges from 0 to 1, is scaled by a multiplication factor of 10,000 to save the image as integer data type to reduce file size. Refer to the class value of the corresponding pixel in the "MICAsummaryimage_2micron_classes" image and the information in columns 7 – 13 of table 2 to determine the best match material and reference spectrum of a pixel. Data are unprojected geographic latitude/longitude (WGS-84). An associated ENVI header file (MICAsummaryimage_2micron_fits.hdr) gives additional details on the file content.
MICAsummaryimage_2micron_fits.hdr	ENVI header file for image file "MICAsummaryimage_2micron_fits.dat"	Text file containing ENVI header information on the image file format.
MICAsummaryimage_2micron_fits.xml	Metadata file for image file "MICAsummaryimage_2micron_fits.dat"	Extensible Markup Language (XML) file describing the image file.
MICAsummaryimage_1micron_depths.dat	Image of overall feature depth values for iron-bearing minerals and other materials detected in the MICA 1-µm analysis	Binary file of signed integer type (Intel byte order). Image values correspond to depth values of the best match reference spectrum in each pixel. From the MICA analysis, the depth value ranges from 0 to 1; however, here the depth has been scaled by a multiplication factor of 10,000 to save the image as integer data type to reduce file size. Refer to the class value of the corresponding pixel in the "MICAsummaryimage_1micron_classes" image and the information in columns 7 – 13 of table 1 to determine the best match material and reference spectrum of a pixel. An associated ENVI header file (MICAsummaryimage_1micron_depths.hdr) gives additional details on the file content.
MICAsummaryimage_1micron_depths.hdr	ENVI header file for image file "MICAsummaryimage_1micron_depths.dat"	Text file containing ENVI header information on the image file format.
MICAsummaryimage_1micron_classes.xml	Metadata file for image file "MICAsummaryimage_1micron_depths.dat"	Extensible Markup Language (XML) file describing the image file.
MICAsummaryimage_2micron_depths.dat	Image of overall feature depth values for carbonates, phyllosilicates, sulfates, altered minerals, and other materials detected in the MICA 2-µm analysis	Binary file of signed integer type (Intel byte order). Image values correspond to depth values of the best match reference spectrum in each pixel. From the MICA analysis, the depth value ranges from 0 to 1; however, here the depth has been scaled by a multiplication factor of 10,000 to save the image as integer data type to reduce file size. Refer to the class value of the corresponding pixel in the "MICAsummaryimage_2micron_classes" image and the information in columns 7 – 13 of table 2 to determine the best match material and reference spectrum of a pixel. An associated ENVI header file (MICAsummaryimage_2micron_depths.hdr) gives additional details on the file content.
MICAsummaryimage_2micron_depths.hdr	ENVI header file for image file "MICAsummaryimage_2micron_depths.dat"	Text file containing ENVI header information on the image file format.
MICAsummaryimage_2micron_depths.xml	Metadata file for image file "MICAsummaryimage_2micron_depths.dat"	Extensible Markup Language (XML) file describing the image file.
wetsoils.shp	Vector file with polygons outlining areas in which mineral identifications may have been affected by moisture in the soil.	Shapefile format. Requires associated files with .shx, .prj, and .dbf extensions for use in GIS software such as ArcGIS.

Table 3. Data files available for download.—Continued

[A '.dat' file extension was added to ENVI image file to work with ArcGIS. ENVI, ENvironment for Visualizing Images; MICA, Material Identification and Characterization Algorithm; µm, micrometer]

Data filename	Description	File format
wetsoils.shx	Associated with the vector file "wetsoils.shp"	
wetsoils.prj	Associated with the vector file "wetsoils.shp"	
wetsoils.dbf	Associated with the vector file "wetsoils.shp"	
wetsoils.xml	Metadata file for vector files "wetsoils.shp" and "wetsoils.evf"	Extensible Markup Language (XML) file describing the vector files.
wetsoil.evf	Vector file with polygons outlining areas in which mineral identifications may have been affected by moisture in the soil.	ENVI vector file format.
mcf_afghan_hymap_1micron_ver2.mcf	MICA command file for the 1-µm image analysis of HyMap data. The command file lists the reference spectra, their corresponding diagnostic features, and material selection thresholds.	Text file in MICA command file format (see Kokaly, 2011).
mcf_afghan_hymap_1micron_ver2_colors.txt	File containing class values, names, and colors for MICA output from the 1-µm image analysis.	Text file.
mcf_afghan_hymap_2micron_ver2.mcf	MICA command file for the 2-µm image analysis of HyMap data.The command file lists the reference spectra, their corresponding diagnostic features, and material selection thresholds.	Text file in MICA command file format (see Kokaly, 2011).
mcf_afghan_hymap_2micron_ver2_colors.txt	File containing class values, names, and colors for MICA output from the 2-µm image analysis.	Text file.

Summary

A rigorous procedure was followed to retrieve surface reflectance; however, complications in reflectance conversion were still encountered. These challenges were a consequence of the vastness of this imaging spectrometer dataset, covering an area of more than 480,000 square kilometers with surface elevations spanning more than 5,000 meters. The long length of the data collection period, the variation in daily acquisition times, changing weather conditions, and sometimes high levels of airborne dust also complicated reflectance retrievals. Thus, further improvement in the reflectance calibration of the HyMap data could possibly be achieved, either through improved radiative transfer correction or incorporation of additional spectra of invariant ground-calibration sites. Future calibration efforts should be targeted at areas in the maps where variation in mapped mineralogy is evident at image tile boundaries.

The surface mineral distributions derived from the HyMap imaging spectrometer data of Afghanistan span the largest terrestrial area characterized by an imaging spectrometer to date. The material maps are being applied to natural resource development and to prioritize areas for further study. These studies are only the initial steps in realizing the potential offered by cutting-edge remote sensing technology in defining mineral distributions to assist in the economic revitalization of Afghanistan. The digital maps described in this report can be downloaded and incorporated into remote sensing and Geographic Information Systems (GIS) software for comparison to other geologic and geophysical data (*http://pubs.usgs.gov/ds/787/downloads/*).

Acknowledgments

Michaela Johnson (USGS) created the metadata files describing the digital data and provided helpful reviews of this manuscript. K. Eric Livo (USGS) provided vital support for the HyMap data collection in Afghanistan. Kathleen Dudek (contractor to USGS) contributed significantly to the processing of the HyMap data.

References Cited

Clark, R. N., 1999, Spectroscopy of rocks and minerals and principles of spectroscopy, *in* Rencz, A.N., ed., Manual remote sensing: New York, John Wiley, p. 3–58.

Clark, R.N., and Roush, T.L., 1984, Reflectance spectroscopy—Quantitative analysis techniques for remote sensing applications: Journal of Geophysical Research, v. 89, p. 6,329−6,340.

Clark, R.N., Gallagher, A. J., and Swayze, G. A., 1990, Material absorption band depth mapping of imaging spectrometer data using a complete band shape least-squares fit with library reference spectra, *in* Green, R.O., ed., Proceedings of the second airborne visible/infrared imaging spectrometer (AVIRIS) workshop: Pasadena, NASA Jet Propulsion Laboratory Publication, v. 90-54, p. 176–186.

Clark, R.N., Swayze, G.A., Livo, K.E., Kokaly, R.F., King, T.V.V., Dalton, J.B., Vance, J.S., Rockwell, B.W., Hoefen, T., and McDougal, R.R., 2002, Surface reflectance calibration of terrestrial imaging spectroscopy data: A tutorial using AVIRIS, *in* Green, R.O., ed., Proceedings of the 10th Airborne Earth Science Workshop: Pasadena, NASA Jet Propulsion Laboratory Publication 02-1.

Clark, R.N., Swayze, G.A., Livo, K.E., Kokaly, R.F., Sutley, S.J., Dalton, J.B., McDougal, R.R., and Gent, C.A., 2003, Imaging spectroscopy—Earth and planetary remote sensing with the USGS Tetracorder and expert systems: Journal of Geophysical Research, v. 108, no. E12, p. 5-1 to 5-44, doi:10.1029/2002JE001847, accessed May 7, 2013, at *http://onlinelibrary.wiley.com/doi/10.1029/2002JE001847/full*.

Clark, R.N., Swayze, G.A., Wise, R., Livo, E., Hoefen, T., Kokaly, R., and Sutley, S.J., 2007, USGS digital spectral library splib06a: U.S. Geological Survey Digital Data Series 231. (Also available at *http://speclab.cr.usgs.gov/spectral.lib06*.)

Cocks, T., Jenssen, R., Stewart, A., Wilson, I., and Shields, T., 1998, The HyMap airborne hyperspectral sensor—The system, calibration and performance, *in* Schaepman, M., Schlapfer, D., and Itten, K.I., eds., Proceedings of the 1st EARSeL Workshop on Imaging Spectroscopy, 6-8 October 1998, Zurich: Paris, EARSeL, p. 37–43.

Davis, P.A., 2007, Landsat ETM+ false-color image mosaics of Afghanistan: U.S. Geological Survey Open-File Report 2007–1029, 22 p.

Elvidge, C.D., 1990, Visible and near infrared reflectance characteristics of dry plant materials: International Journal of Remote Sensing, v. 11, p. 1,775−1,795.

Ingle, J. D., 1988, Spectrochemical analysis: Engelwood Cliffs, New Jersey, Prentice-Hall, p. 424– 425.

ITT Visual Information Solutions, 2009, ENVI 4.7/ IDL version 7.1.1 user's guide: Boulder, Colorado, ITT Visual Information Solutions.

King, T.V.V., Kokaly, R.F., Hoefen, T.M., Dudek, K.B., and Livo, K.E., 2011a, Surface materials map of Afghanistan—Iron-bearing minerals and other materials: U.S. Geological Survey Scientific Investigations Map 3152–B, one sheet, scale 1:1,100,000. (Also available at *http://pubs.usgs.gov/sim/3152/B/*.)

King, T.V.V., Johnson, M.R., Hubbard, B.E., and Drenth, B.J., eds., 2011b, Identification of mineral resources in Afghanistan—Detecting and mapping resource anomalies in prioritized areas using geophysical and remote sensing (ASTER and HyMap) data: U.S. Geological Survey Open-File Report 2011–1229, 327 p.

Kokaly, R.F., 2011, PRISM—Processing routines in IDL for spectroscopic measurements (installation manual and user's guide, version 1.0): U.S. Geological Survey Open-File Report 2011–1155, 432 p. (Also available at *http://pubs.usgs.gov/of/2011/1155/*.)

Kokaly, R.F., Despain, D.G., Clark, R.N., and Livo, K.E., 2003, Mapping vegetation in Yellowstone National Park using spectral feature analysis of AVIRIS data: Remote Sensing of Environment, v. 84, p. 437–456.

Kokaly, R.F., Despain, D.G., Clark, R.N. and Livo, K.E., 2007a, Spectral analysis of absorption features for mapping vegetation cover and microbial communities in Yellowstone National Park using AVIRIS data, *in* Morgan, L.A., ed., Integrated geoscience studies in the greater Yellowstone area—Volcanic, tectonic, and hydrothermal processes in the Yellowstone geoecosystem: U.S. Geological Survey Professional Paper 1717, 532 p.

Kokaly, R.F., Rockwell, B.W., Haire, S.L., and King, T.V.V., 2007b, Characterization of postfire surface cover, soils, and burn severity at the Cerro Grande Fire, New Mexico, using hyperspectral and multispectral remote sensing: Remote Sensing of Environment, v. 106, p. 305−325.

Kokaly, R.F., King, T.V.V., and Livo, K.E., 2008, Airborne hyperspectral survey of Afghanistan 2007—Flight line planning and HyMap data collection: U.S. Geological Survey Open-File Report 2008–1235, 14 p. (Also available at *http://pubs.usgs.gov/of/2008/1235/*.)

Kokaly, R.F., Asner, G.P., Ollinger, S.V., Martin, M.E., and Wessman, C.A., 2009, Characterizing canopy biochemistry from imaging spectroscopy and its application to ecosystem studies: Remote Sensing of Environment, v. 113, p. 78–91.

Kokaly, R.F., and Giles, S.A., 2011, Analysis of imaging spectrometer data for the Panjsher Valley area of interest, Afghanistan, chap. 13B *of* Peters, S.G., King, T.V.V., Mack, T.J., and Chornack, M.P., eds., and the U.S. Geological Survey Afghanistan Mineral Assessment Team, 2011, Summaries of important areas for mineral investment and production opportunities of nonfuel minerals in Afghanistan: U.S. Geological Survey Open-File Report 2011–1204, p. 1,017-1,045.

Kokaly, R.F., King, T.V.V., Hoefen, T.M., Dudek, K.B., and Livo, K.E., 2011, Surface materials map of Afghanistan—Carbonates, phyllosilicates, sulfates, altered minerals, and other materials: U.S. Geological Survey Scientific Investigations Map 3152–A, one sheet, scale 1:1,100,000. (Also available at *http://pubs.usgs.gov/sim/3152/A/*.)

Peters, S.G., Ludington, S.D., Orris, G.J., Sutphin, D.M., and Bliss, J.D., eds., 2007, Preliminary non-fuel mineral resource assessment of Afghanistan: U.S. Geological Survey Open-File Report 2007–1214, 810 p.

Peters, S.G., King, T.V.V., Mack, T.J., and Chornack, M.P., eds., and the U.S. Geological Survey Afghanistan Mineral Assessment Team, 2011, Summaries of important areas for mineral investment and production opportunities of nonfuel minerals in Afghanistan: U.S. Geological Survey Open-File Report 2011–1204, 1,810 p. plus appendixes on DVD. (Also available at *http://pubs.usgs.gov/of/2011/1204/*).

U.S. Geological Survey, 2005, Afghanistan geospatial reference datasets: U.S. Geological Survey database, accessed May 7, 2013, at *http://afghanistan.cr.usgs.gov/geospatial-reference-datasets*.

Publishing support provided by:
Denver Publishing Service Center
Rolla Publishing Service Center

For more information concerning this publication, contact:
Center Director, USGS Crustal Geophysics and Geochemistry Science Center
Box 25046, Mail Stop 964
Denver, CO 80225
(303) 236-1312

Or visit the Crustal Geophysics and Geochemistry Science Center Web site at:
http://crustal.usgs.gov/